Mercury cycling in a flooded rice paddy

Sarah E. Rothenberg[1,2] and Xinbin Feng[1]

Received 2 July 2011; revised 9 May 2012; accepted 10 May 2012; published 3 July 2012.

[1] In 2008 and 2009, mercury (Hg) cycling was investigated in a flooded rice paddy in the Wanshan Hg mining region of eastern Guizhou, China, in the rice-planted (2008 and 2009) and fallow (2009) sections of the same paddy. In the rice-planted section, pore water was more acidic and pore water methylmercury (MeHg) concentrations were higher compared to the fallow section. However, iron (Fe) and sulfur (S) cycling differed in 2008 and 2009, with higher sediment Fe concentrations in 2009, when pore water MeHg and sulfate concentrations were more strongly correlated in the rice-planted section. We explored whether elevated sediment Fe contributed to S cycling and hence, Hg(II)-methylation. Critical pH values for formation of $FeS_{(s)}$ were estimated. Based on pore water pH collected in both sections of the paddy, the fallow section was more often a sink for $FeS_{(s)}$, while $FeS_{(s)}$ did not form in the rice-planted section, although sulfide concentrations were low in both sections in both years (i.e.,<10 μM). We hypothesized Fe(III) oxidized sulfide, and intermediate S species (e.g., polysulfides) were further oxidized to sulfate instead of forming $FeS_{(s)}$, thus prolonging sulfate reduction and promoting Hg(II)-methylation in the rice-planted section in 2009. Results suggested Fe(III) reduction increased electron acceptors for sulfate-reducing bacteria, which indirectly enhanced Hg(II)-methylation. Additionally, highest sediment MeHg concentrations were observed in the fallow section after the paddy was dried and re-wetted, indicating water-saving rice cultivation practices (e.g., alternating wetting and drying), may cause MeHg concentrations in paddy soil to spike, which should be further investigated.

Citation: Rothenberg, S. E., and X. Feng (2012), Mercury cycling in a flooded rice paddy, *J. Geophys. Res.*, *117*, G03003, doi:10.1029/2011JG001800.

1. Introduction

[2] China is the world's highest emitter of anthropogenic mercury (Hg) due to reliance on more than 2000 coal-burning power plants to fuel industrial growth [*Pacyna et al.*, 2010]. China is also the global leader in paddy rice cultivation, producing 29% of the world's rice supply in 2009 (World Rice Statistics, http://irri.org/our-science/targeting-and-policy/world-rice-statistics). Like other submerged wetlands [e.g., *St. Louis et al.*, 1994], irrigated lowland flooded rice paddies are active Hg(II)-methylation sites, converting inorganic Hg (II) to more toxic methylmercury (MeHg), which may be accumulated in rice grain [*Feng et al.*, 2008; *Horvat et al.*, 2003; *Rothenberg et al.*, 2011, 2012; *Shi et al.*, 2005; *Zhang et al.*, 2010]. Half the global population subsists on rice as a staple food; therefore, it is critical to investigate biogeochemical controls on Hg cycling in rice paddies.

[3] The primary methylators of inorganic Hg(II) in anoxic sediment are sulfate-reducing bacteria (SRB) [*Compeau and Bartha*, 1985; *Gilmour et al.*, 1992] and iron-reducing bacteria (FeRB) [*Fleming et al.*, 2006; *Kerin et al.*, 2006], which compete with other microbes in the vicinity of rice roots for electron donors [*Achtnich et al.*, 1995; *Scheid et al.*, 2004]. FeRB outcompete SRB in sediment nearly depleted of electron donors due to a lower threshold for utilization of acetate and hydrogen [*Lovley and Phillips*, 1987a], while both processes overlap in paddy soil where electron donors are not limiting [*Achtnich et al.*, 1995; *Lovley and Phillips*, 1987a].

[4] A number of mechanisms persist in flooded rice paddies, helping rice plants thrive, which may influence microbial Hg(II)-methylation. For example, in waterlogged soil, aerenchyma tissue allows the diffusion of oxygen (O_2) from the rice root apex into the rhizosphere, creating an oxic zone at depth that is distinct from the surrounding bulk soil [*Colmer*, 2003]. O_2 oxidizes sulfide, which is toxic to rice plants [*Fairhurst et al.*, 2007]. Regeneration of sulfate (SO_4^{2-}) increases electron acceptors for SRB, while low sulfide levels increase the mole fraction of $HgS^{o}_{(aq)}$, which is considered more bioavailable for Hg(II)-methylation by SRB, creating conditions favorable for MeHg production under a passive diffusion model [*Benoit et al.*, 1999, 2001].

[1]Institute of Geochemistry, State Key Laboratory of Environmental Geochemistry, Chinese Academy of Sciences, Guiyang, China.
[2]Department of Environmental Health Sciences, The Arnold School of Public Health, University of South Carolina, Columbia, South Carolina, USA.

Corresponding authors: X. Feng, Institute of Geochemistry, State Key Laboratory of Environmental Geochemistry, Chinese Academy of Sciences, 46 Guanshui Road, Guiyang 550002, China. (fengxinbin@vip.skleg.cn)
S. E. Rothenberg, Department of Environmental Health Sciences, The Arnold School of Public Health, University of South Carolina, PHRC Room 401C, 921 Assembly St., Columbia, SC 29208, USA. (rothenberg.sarah@sc.edu)

0148-0227/12/2011JG001800

Lower pH in the rhizosphere may also enhance Hg cycling in the vicinity of rice roots. Sources of acidity include formation of Fe-plaque around the roots, a process that releases protons:

$$4\,Fe(II) + O_2 + 10\,H_2O \rightarrow 4\,Fe(OH)_3 + 8\,H^+ \quad (1)$$

and pH may be 1–2 log units lower compared to the surrounding bulk soil [*Begg et al.*, 1994]. Acidity is also generated following uptake of ammonium (NH_4^+), the dominant form of nitrogen in submerged soil, and rice roots export H^+ to maintain neutrality in the roots [*Begg et al.*, 1994]. An inverse relationship between pH and MeHg levels is well-established in surface waters [*Bloom et al.*, 1991; *Rothenberg et al.*, 2008], and between lake water and fish tissue [*Spry and Wiener*, 1991], which may be due to higher bioavailability of $HgS^o_{(aq)}$ at lower pH [*Rothenberg et al.*, 2008], or increased facilitated uptake of inorganic Hg(II) into the bacterial cell at lower pH [*Kelly et al.*, 2003; *Golding et al.*, 2008], or higher solubility of inorganic Hg(II) at lower pH [*Haitzer et al.*, 2003].

[5] In 2008 and 2009, Hg cycling was characterized in a rice paddy in eastern Guizhou province, China, located in a village on the opposite side of the mountain where the Wanshan Hg mine was excavated. Our primary aim was to investigate whether Hg cycling and MeHg production reflected processes occurring on a longer time scale (throughout the rice-growing season) or a shorter time scale (within hours), or both. Our secondary aim was to determine the effect of rice roots on Hg (II)-methylation within in a flooded rice paddy. To address these aims, sediment and pore water samples (0–18 cm depth) were collected from the rice-planted section (in 2008 and 2009) and fallow section (in 2009) of the same rice paddy at 3–4 time points spaced 2–3 weeks apart. Controls on Hg cycling were quantified, including concentrations of pore water sulfide, SO_4^{2-}, and Fe, and sediment acid-volatile sulfides (AVS), Fe and organic content. For greater temporal resolution, pore water samples (0–2 cm depth) were collected every three hours throughout a 24-h period (in 2008 and 2009) in the rice-growing section of the paddy to examine diel trends in Hg cycling. Lastly, in 2008 and 2009 pH and temperature sensors were embedded in the soil subsurface, and data were stored in 10-min intervals for 53 and 63 days, respectively. Temperature and pH sensors are widely available for environmental monitoring, and both parameters are related to Hg(II)-methylation [*Ullrich et al.*, 2001].

2. Methods

2.1. Location

[6] All samples in both years were collected from the same rice paddy, located in Gouxi village in the region of the former Wanshan Hg mine, where subsistence rice farming is practiced. Although the Wanshan Hg mine was officially closed in 2002, mine tailings (i.e., Hg cinnabar, $HgS_{(s)}$) and other Hg waste are transported to the surrounding villages and smelted in crude ovens. Smelting releases fugitive Hg emissions, which are deposited through wet and dry deposition to the surrounding rice paddies [*Li et al.*, 2009]. The rice paddy was located downwind from at least one Hg smelter, which was occasionally active during the summer. In this region, terraced rice paddies are carved into the mountainside, where bedrock begins at <1 m depth; therefore, there is no interface between paddy water and groundwater. In both years, the paddy was flooded during the last week of May, and rice seedlings were transplanted to submerged paddies approximately 20 days after flooding (DAF) with a density of 12–15 rice plants per m^2. The planting density was lower than typically used at the Guizhou Rice Research Institute (16–25 rice plants per m^2, Junmei You, Guizhou Rice Research Institute, personal communication). Once flooded, standing water (5–10 cm depth) was stored on the field throughout the rice-growing season. All rice paddies in the village were connected through a series of channels, and received water through precipitation or runoff from the next highest paddy (i.e., seepage). Water loss from the paddy occurred through evaporation or seepage but not percolation (i.e., downward flow).

2.2. Sampling Design

[7] In 2008 the paddy was planted with rice, and in 2009 one-fourth of the paddy remained fallow (i.e., devegetated) for comparison between the two sections (2008 rice-planted: 11 m × 17 m; 2009 rice-planted: 11 m × 13 m; 2009 fallow: 11 m × 4 m). All plant growth, including algae, was cleared by hand in the fallow section at the start of the season (i.e., 32 DAF), and then every ~20 days (54, 75, and 94 DAF) to ensure the fallow section remained fallow. The sampling approach described was the same for both sections. In 2008 pore water temperature and pH sensors were deployed between 22 July–13 September (58–111 DAF), and in 2009 sensors were deployed between 25 June–27 August (32–95 DAF). For depth profiles, in 2008 sediment cores were collected on 24 July, 9 August, and 29 August (i.e., 60, 76 and 96 DAF), and in 2009 sediment cores were collected on 25 June, 17 July, 7 August, and 27 August (i.e., 32, 54, 75, and 94 DAF) (see Section 2.4 for more details on sediment cores). Surface water samples from the rice paddy were collected at the same time as sediment cores. Sampling dates roughly corresponded to the following growth stages for rice: tillering or vegetative stage (32 DAF), late-tillering and panicle initiation (54–60 DAF), panicle initiation/flowering (75–76 DAF), and grain filling (94–96 DAF), while final ripening occurred after the rice paddy was drained (95–111 DAF) [*Fairhurst et al.*, 2007].

[8] To characterize diurnal cycling of Hg species, at the end of the rice maturation phase during the grain-filling period (94–96 DAF), sediment cores were extracted from the rice-planted section every 3 h over a 24-h period (28–29 August 2008: 09:30–09:30; 26–27 August 2009: 14:30–14:30) (n = 9 time points each year), and total Hg (THg) and MeHg concentrations were analyzed in pore water (0–2 cm depth). In 2009, the fallow section was too dry to extract sediment cores at the start of the 24-h study.

2.3. Cleaning

[9] All glassware, centrifuge tubes and sediment cores were soaked overnight in 5% bleach, triple-rinsed with distilled, deionized-H_2O (DDI-H_2O, resistivity: 18.2 MΩ), then soaked overnight in 20% nitric acid (HNO_3^-) and triple-rinsed with DDI-H_2O, then double-bagged. Glassware was also heated up to 1 h at 500°C to ensure thermal desorption of Hg, cooled and then double-bagged.

2.4. Field Sampling

[10] For pore water and sediment depth profiles, triplicate cores were collected at each time point in the paddy within ~0.25 m^2 area, retaining surface water in the headspace to preserve anoxia, sealed with rubber stoppers, double-bagged, and stored on ice or refrigerated (in the dark) until cores were processed at the Institute of Geochemistry in Guiyang (within 36–48 h after collection from the paddy). The two longest cores were extruded under N_2 gas in a glove bag (Atmos, Sigma Aldrich, St. Louis, Mo.) into 50-mL centrifuge tubes (sliced every 2 cm, up to 18 cm), which were centrifuged outside the glove bag (3500 rpm, 30 min), then returned to the glove bag where pore water was filtered (0.22 μM syringe filter, nylon material) and composited into 100-mL borosilicate glass bottles to ensure sufficient pore water volume for all analyses. Aliquots were removed for analysis of Fe species, total sulfide [$(H_2S)_T$], SO_4^{2-}, and MeHg. Remaining pore water was acidified (0.5% HCl) for analysis of THg, double-bagged and refrigerated in the dark until analysis. In the glove bag, MeHg samples were diluted (usually 9:1 DDI-H_2O:sample) in 50-mL centrifuge tubes, preserved with 0.5% HCl, double-bagged, and frozen (−26°C). Aliquots for pore water $(H_2S)_T$ and Fe species were preserved in the glove bag and analyzed immediately (see Sections 2.6 and 2.8, respectively), and aliquots for SO_4^{2-} were refrigerated unpreserved. The methods described for collection, extrusion and preservation of pore water Hg species for depth profiles were the same as those used for the 24-h sampling, except duplicate sediment cores were collected every three hours (n = 9 time points) and pore water (0–2 cm depth) was composited from both cores. In the rice paddy, surface water samples were filtered (0.22 μM syringe filter, nylon material) directly into duplicate 100-mL borosilicate bottles, and one bottle was preserved in the field (0.5% HCl) for analysis of Hg species, while the other bottle was refrigerated unpreserved for analysis of SO_4^{2-}. A 45-mL aliquot from the former bottle was poured into a 50-ml centrifuge tube, double-bagged and frozen for MeHg analysis. Sediment in 50-mL centrifuge tubes was frozen (−26°C) for analysis of THg, MeHg, Fe, AVS and organic content. Pore water and surface water THg analyses were usually completed the week following sampling, while remaining analyses were completed within 6 months.

2.5. THg and MeHg Analyses

[11] Pore water and surface water MeHg and THg concentrations were analyzed following U.S. EPA Method 1630 [*U.S. Environmental Protection Agency* (*EPA*), 2001] and U.S. EPA Method 1631 [*EPA*, 2002], respectively. For THg, samples were digested at least 12 h after addition of 0.5% (v/v) 0.2 N bromine monochloride, then pre-reduced using 0.3% hydroxylamine hydrochloride. Hg(II) was further reduced to Hg(0) with stannous chloride, and quantification was by gold amalgamation/cold vapor atomic fluorescence spectrometry (CVAFS) (Tekran Model 2500 Hg Analyzer, Knoxville, Tenn.). For MeHg, acidified samples were distilled into 40-mL receiving vials. Sample pH was adjusted to 4.9 using 2 M acetate buffer, then ethylated using 1% sodium tetraethylborate, converting nonvolatile MeHg to gaseous methylethylmercury, which was purged onto Tenax traps, then thermally desorbed and decomposed by gas chromatography and pyrolysis, converting organo Hg forms to Hg(0), and then quantification by CVAFS (Brooks Rand Model III, Seattle).

[12] In 2008 sediment THg levels were analyzed following acid digestion (5 mL of concentrated HNO_3^- + hydrochloric acid (HCL), 1:3 v/v), heating in a water bath at 95°C for 5 min, addition of 0.2 N bromine monochloride, heating at 95°C for 30 min, then the same Hg-reduction steps followed for aqueous samples, and quantification using CVAFS. In 2009 solid-phase THg samples were analyzed with a portable Hg vapor analyzer (Lumex, Model RA-915+/PYRO-915+, St. Petersburg, Russia), using methods described in U.S. EPA Method 7473 [*EPA*, 2007] involving thermal decomposition, amalgamation and atomic absorption spectrophotometry, and no pre-digestion steps were required. The two methods (1631[*EPA*, 2002] and 7473 [*EPA*, 2007]) were previously compared, and the correlation (r) was 0.78 for 17 samples [*Rothenberg et al.*, 2010]. In 2008 and 2009 sediment MeHg concentrations were analyzed following solvent extraction with dichloromethane (CH_2Cl_2) to minimize matrix interferences [*Liang et al.*, 2004]. Sediment samples were leached in 1.5 ml 1 M copper-sulfate, 7.5 mL 25% HNO_3 and 10 mL CH_2Cl_2 [*Liang et al.*, 2004], followed by vigorous shaking, centrifugation (3500 RPM, 25 min), separation of the organic phase, back extraction into DDI-H_2O, and heating in a 50°C water bath to drive off CH_2Cl_2. MeHg was then analyzed following ethylation, collection onto Tenax traps, and separation and quantification using gas chromatography-CVAFS [*EPA*, 2001]. Quality assurance and control (QA/QC), including percent recovery, relative percent difference (RPD) between duplicate or triplicate analyses, and minimum detection levels (MDL) are reported in Table 1. THg and MeHg method blanks averaged 1.7 ng/L and <detection level, respectively.

2.6. Analysis of Total Sulfide $(H_2S)_T$

[13] $(H_2S)_T$, defined as the sum of $H_2S + HS^- + S^{2-}$, was analyzed using iodometry and methylene blue (667 nm) [*Cline*, 1969]. In 2008, pore water samples were extracted from sediment cores in a glove bag under N_2 gas at the Institute of Geochemistry (see Section 2.4), and analyzed immediately. In 2009, pore water samples for analysis of $(H_2S)_T$ were collected using both sediment cores and in situ dialysis membrane devices ("peepers"); the latter were processed in the field. Prior to deployment, peepers were filled with deoxygenated DDI-H_2O and sealed with a 0.2 μM membrane, then deployed on 25 June, 17 July, and 7 August (i.e., 32, 54, and 75 DAF) in the rice-planted and fallow sections of the paddy, and retrieved after 21, 22 and 20 days deployed, respectively. After removal from paddy soil, the external parts of the peepers were quickly rinsed in distilled H_2O bubbled with N_2 to remove dirt, then put directly into a glove bag (Atmos, Sigma Aldrich, St. Louis, Mo.), which was then flushed three times with N_2. Pore water (3 mL) was extracted from each peeper cell using syringes and injected directly into prepared 30-mL serum bottles. Serum bottles were pre-filled with Cline's reagents, sealed with butyl rubber stoppers and aluminum seals, and the headspace was purged with N_2 for 30 s. Pore water was extracted in the field and analyzed after returning to the Institute of Geochemistry. Detection levels were based on the region of the standard curve where there was a significant change in

Table 1. QA/QC Data for THg and MeHg Analyses[a]

	Aqueous THg	Solid-Phase THg	Aqueous MeHg	Solid-Phase MeHg
Recovery (%)	101 (n = 3)	102 (n = 6)	89 (n = 27)	86 (n = 8)
RPD (%)	7.4 (n = 92)	14 (n = 74)	27 (n = 11)	24 (n = 9)
MDL	0.71 ng/L	2.5 ng/g	0.056 ng/L	0.075 ng/g

[a]Data includes percent recovery of matrix spikes (for surface water and pore water) or standard reference material (for sediment); relative percent difference (RPD), here defined as 100 times the ratio between the standard deviation and the average of duplicate or triplicate analyses; the sample size (n); and the method detection level (MDL). Sediment standard reference material included GBW07405 (GSS5) and NIST Montana Soil (2710) for THg, and IRMM-BCR 580 for MeHg.

sensitivity, including 1.3 μM and 0.10 μM in 2008 and 2009, respectively.

2.7. Acid-Volatile Sulfides (AVS)

[14] AVS was analyzed in 2009 in the rice-planted and fallow sections. Archived sediment was digested for 1 h in 1 N HCl, while bubbling with N_2, and $(H_2S)_T$ was trapped by two flasks in series, each with 40 mL 0.3 M zinc acetate and 0.12 M sodium acetate [*Allen et al.*, 1993], and $(H_2S)_T$ was measured in each flask by methylene blue as described in Section 2.6 [*Cline*, 1969].

2.8. Analysis of HCl-Extractable Fe Species and SO_4^{2-}

[15] Pore water 0.5 N HCl-extractable Fe(II) was measured using the ferrozine method (562 nm) [*Lovley and Phillips*, 1987b]. HCl-extractable FeT, defined as the sum of HCL-extractable Fe(II) + Fe(III) was quantified after reduction by hydroxylamine hydrochloride [*Gibbs*, 1979]. Sediment HCl-extractable Fe(II) and FeT were determined in archived sediment after 1 h digestion in 1 N HCl, while bubbling with N_2. HCl-extractable Fe(III) was calculated as the difference between HCl-extractable FeT and Fe(II). Surface water and pore water SO_4^{2-} was measured by ion chromatography.

2.9. Wet: Dry Ratio and Organic Matter (OM)

[16] Sediment was added to pre-weighed crucibles and dried overnight at 60°C, then weighed for determination of the wet: dry ratio. Samples were then ignited at 550°C for 2 h and the percent loss on ignition (%LOI) was determined for organic content (Method 2540-E [*Standard Methods Committee*, 1998]). Results for sediment THg, MeHg, HCl-extractable Fe and AVS concentrations are reported in dry weight.

2.10. pH Electrode Deployment

[17] Continuous pore water pH measurements were monitored near the soil surface using combination pH electrodes (Model P14, Sentek Ltd., Braintree, UK), and data were stored in 10-min intervals on Campbell data loggers (Model CR800, Campbell Scientific, Logan, Utah). In 2008 pH electrodes were connected directly to data loggers, and in 2009 pH preamplifiers were inserted between pH sensors and data loggers (PHAMP-1, Sensorex Corp., Garden Grove, Calif.) to reduce electrode impedance signals. Each data logger and accompanying battery pack was stored individually in a junction box or plastic box with 10–20 g dessicant, which was changed every 2–3 weeks.

[18] In 2008 4 pH electrodes were deployed in the center of the rice paddy for 53 days (22 July–13 September, corresponding to 58–111 DAF). In 2009, one-fourth of the paddy remained fallow, and 2 pH electrodes were deployed in the rice-planted and fallow sections for 63 days (4 sensors total) (rice-planted/fallow: 25/24 June–27/26 August, corresponding to 32–95 DAF and 31–94 DAF, respectively). pH electrodes were deployed in pairs in a slotted PVC pylon (Gossco Manufacturing, Fullerton, Calif.), which allowed pore water to infiltrate the pylon from 0 to 16 cm depth but the pylon was otherwise water-tight (specifications for pylon construction from T. Harmon, UC Merced, personal communication).

2.11. pH Electrode Calibration

[19] pH electrodes were calibrated in the laboratory (25°C) 1–2 days before and 2–3 days after deployment using 3 pH standards (Table 2). A temperature correction factor was applied based on the Nernst equation (i.e., for every 10°C change in temperature between pore water and the calibration solution, pH is expected to change by 0.03 units per log unit from pH 7), using temperature data measured simultaneously in 10-min intervals (see Section 2.12). Data logger output (mV) for each pH electrode was converted to pH log units using both pre- and post-calibration curves, then temperature-corrected using the Nernst equation, and results for each pair of pH electrodes were averaged. In 2008 two sensors (out of 4) could not be calibrated at the end of the deployment (electrodes 2 and 3), and average pore water pH levels were based on data from the 2 remaining functioning sensors (electrodes 1 and 4) (Table 2). In 2009 in the

Table 2. Pre- and Post-Deployment Calibration Results for pH Sensors[a]

Year	Site	pH Sensor (#)	Pre-Calibration	Post-Calibration	n	Δ Slope/Day (%/Day)
2008	Rice-planted	1[b]	y = −56.6x + 364	y = −54.8x + 359	7581	−0.060
	Rice-planted	2[b]	y = −56.2x + 370	NA	NA	NA
	Rice-planted	3[c]	y = −55.8x + 353	NA	NA	NA
	Rice-planted	4[c]	y = −58.8x + 403	y = −54.3x + 357	7460	−0.15
2009	Fallow	9[d]	y = −58.1x + 403	y = −51.2x + 357	8967	−0.19
	Fallow	10[d]	y = −58.2x + 405	y = −54.1x + 378	8967	−0.11
	Rice-planted	11[e]	y = −58.3x + 414	y = −24.8x + 186	8928	−0.90
	Rice-planted	12[e]	y = −58.8x + 415	y = −54.8x + 449	8928	−0.11

[a]Here the dependent variable (y) represents the data logger reading (mV), the independent variable (x) is the pH standard (pH 4.003, pH 6.864, and pH 9.182), and n represents the number of sampling points. Statistics include the change in calibration slope (Δ slope/day). The regression coefficients (r^2) ranged between 0.998 and 1.00 for all calibrations. NA refers to unobtainable results.
[b–e]Matching superscripts indicate that sensors were housed in the same pylon.

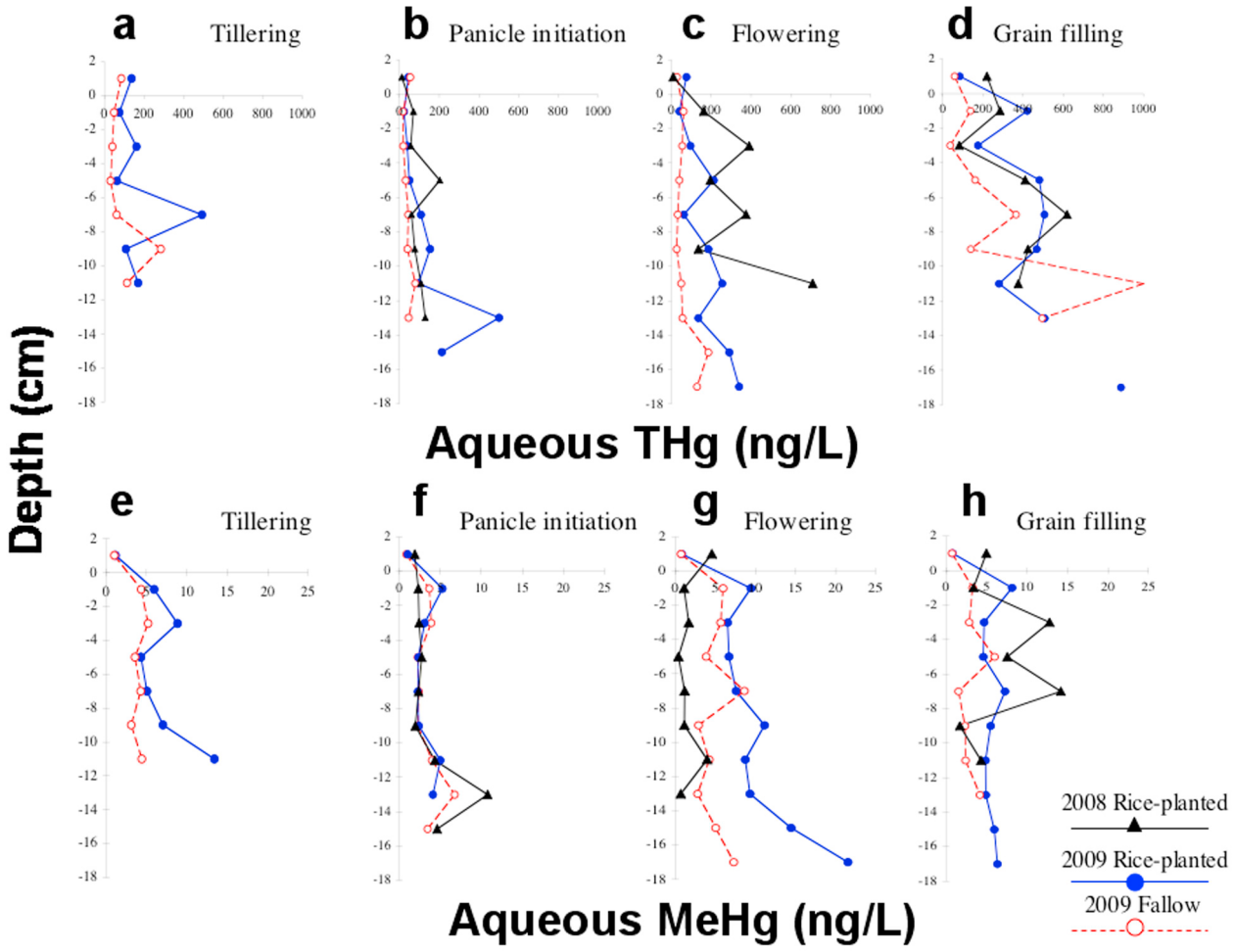

Figure 1. Depth profiles of surface water and pore water concentrations of THg (ng/L) (a–d) and MeHg (ng/L) (e–h).

rice-planted section, 1 sensor (out of 2) lost sensitivity (electrode 11), which was restored post-deployment. For this site, pore water pH levels were averaged using the pre-calibration results for electrode 11, and pre/post calibration results for electrode 12, although results were similar when only electrode 12 was used (electrode 11, 12: pH 6.05, electrode 12: 6.11).

[20] Before deployment, regression slopes for all 8 sensors were within 94–99% of the Nernst value (59.16 mV per pH unit), and post-deployment slopes for 5 of the 8 sensors were within 86–93% of the Nernst value (Table 2). Slopes for electrodes 9–12 were restored to within 95–97% of the Nernst value following cleansing with pH 4 standard, indicating accumulation of particles reduced sensitivity during the deployment. These results underscore the importance of in-field post-deployment calibrations.

[21] Independent field calibrations were used to verify pH sensor readings, including 1) extraction of pore water by syringe near the deployed sensor, 2) comparison of readings between sensors and another pH meter, and 3) pH measurement for pore water extracted from additional sediment cores (as described in Section 2.3, but processed under aerobic conditions). The ratio between independent readings and pH sensor readings ranged from 0.79 to 1.04, and the most reliable method was method #3 (ratio: 1.00–1.02). Differences between methods possibly reflected positioning of the sensor, or issues related to temperature or alkalinity.

2.12. Deployment of Temperature Sensors

[22] In 2008 and 2009, temperature sensors (TMC6-HD, Onset Computer, Pocasset, Mass.) connected to Hobo U12 data loggers (MicroDAQ, Contoocook, N. H.) were deployed in slotted pylons (0–16 cm depth), and data were collected in 10-min intervals for the same timeframe as pH electrodes. In 2008, 2 temperature sensors were deployed (within 1 m^2) and average RPD was 0.52%. In 2009, 1 temperature sensor was deployed in the rice-planted section, and another in the fallow section.

2.13. Statistics

[23] Univariate and bivariate relationships were explored through histograms and two-way scatterplots. To compare differences between groups, paired t-tests were and one-way analysis of variance (ANOVA) with the Sidak multiple-comparison test were used ($\alpha = 0.05$). Simple linear regression and the F test were used to determine significance at the $\alpha = 0.05$ level. Environmental data are often skewed right (mean≫median), and the $\log_{10}$-transformation is applied to

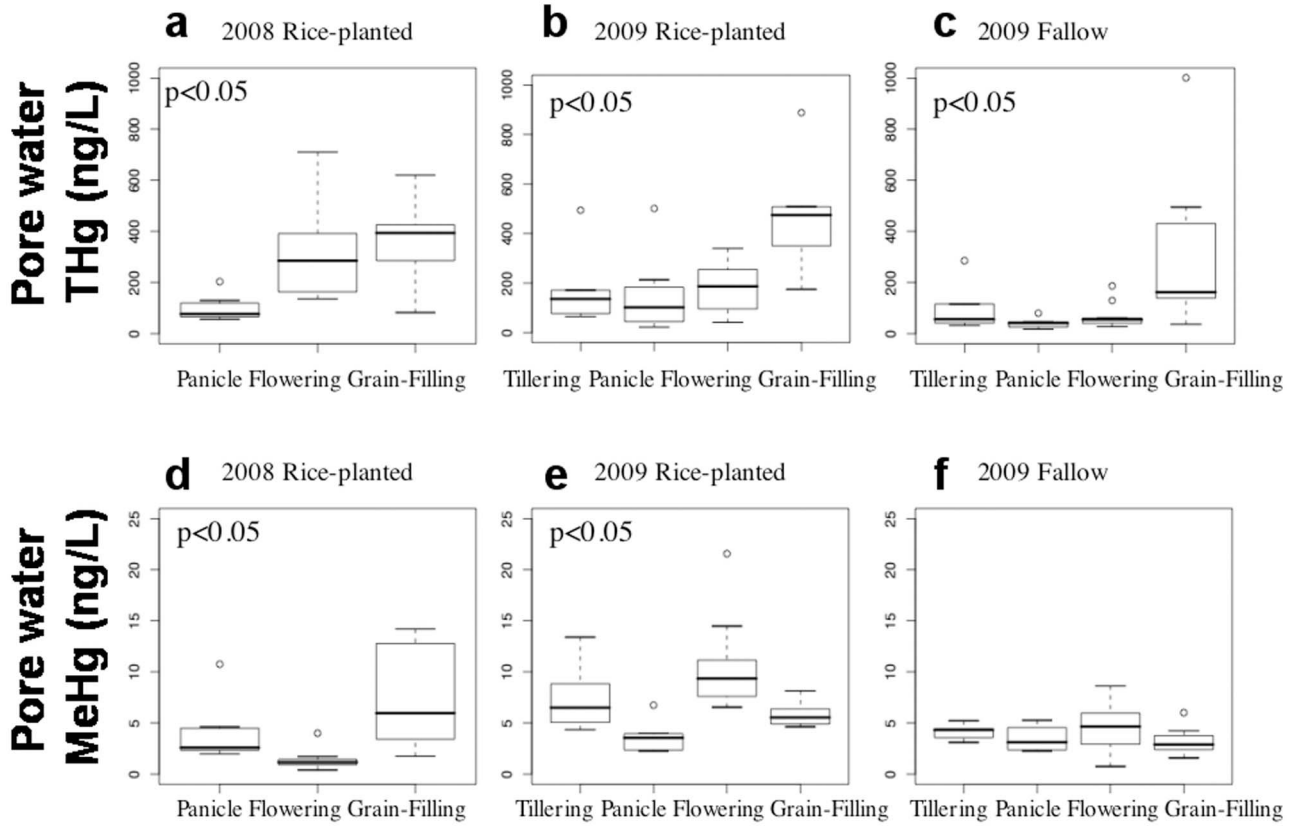

Figure 2. Boxplots for pore water concentrations of THg (ng/L) (a–c) and MeHg (ng/L) (d–f) aggregated for each time point when samples were collected (i.e., tillering, panicle initiation, flowering and grain-filling). A significant difference between at least one pair of time points within each boxplot is denoted with $p < 0.05$ (using ANOVA).

transform skewed data to normality (for this data set, kurtosis ranged between 2.7 and 16). Skewness was assessed visually. When data were $\log_{10}$-transformed, results were reported for both the transformed and raw data. The Stata package (Version 9.2, College Station, Texas) was used for all statistical analyses and regression diagnostics (e.g., residual plots and Cook's distance).

3. Results

3.1. Surface Water and Pore Water THg and MeHg Levels

[24] In 2008 and 2009 surface water and pore water THg levels in the rice-planted section averaged 230 ± 190 ng/L (n = 22 observations) and 230 ± 200 ng/L (n = 35 observations), respectively, and in 2009 in the fallow section THg levels averaged 120 ± 190 ng/L (n = 33 observations) (Figures 1a–1d). Surface water and pore water THg levels were significantly higher in the rice-planted section in both years compared to the fallow section (ANOVA, $p < 0.05$ when data were $\log_{10}$-transformed; ANOVA, $p > 0.30$ for raw data). Lower average THg levels in the fallow section likely reflected spatial differences.

[25] In 2008 and 2009 surface water and pore water MeHg levels in the rice-planted section averaged 4.1 ± 3.7 ng/L (n = 24 observations) and 6.3 ± 4.2 ng/L (n = 36 observations), respectively, and in 2009 in the fallow section aqueous MeHg levels averaged 3.7 ± 1.9 ng/L (n = 33 observations) (Figures 1e–1h). MeHg trends with sediment depth were surprisingly similar in 2008 and 2009 in both sections of the paddy (54 and 60 DAF, Figure 1f), corresponding to panicle initiation. In 2009, average MeHg levels in the overlying surface water were nearly equal between the rice-planted and fallow sections of the paddy (rice-planted: 0.91 ± 0.17 ng/L; fallow: 0.89 ± 0.15 ng/L), but were significantly higher in the pore water (i.e.,<0 cm depth) in the rice-planted section on three of the four sampling events (rice-planted: 6.9 ± 4.0 ng/L; fallow: 4.1 ± 1.6 ng/L; paired t-test, $p < 0.001$ for raw and $\log_{10}$-transformed data) (Figures 1e–1h), suggesting higher Hg(II)-methylation and/or lower retention of MeHg in the soil subsurface. Results from this side-by-side comparison in 2009 were consistent with *Windham-Myers et al.* [2009], who reported devegetation decreased MeHg production in a suite of wetland settings, including three rice paddies.

3.2. Changes in Pore Water THg and MeHg Levels Over the Rice-Growing Season

[26] Data for pore water (<0 cm depth) THg and MeHg levels were aggregated for each sampling date (tillering, panicle initiation, flowering and grain-filling periods) for each year (2008 and 2009) and for the rice-planted and fallow sections of the paddy (Figure 2). THg and MeHg pore water levels were significantly different for at least one sampling

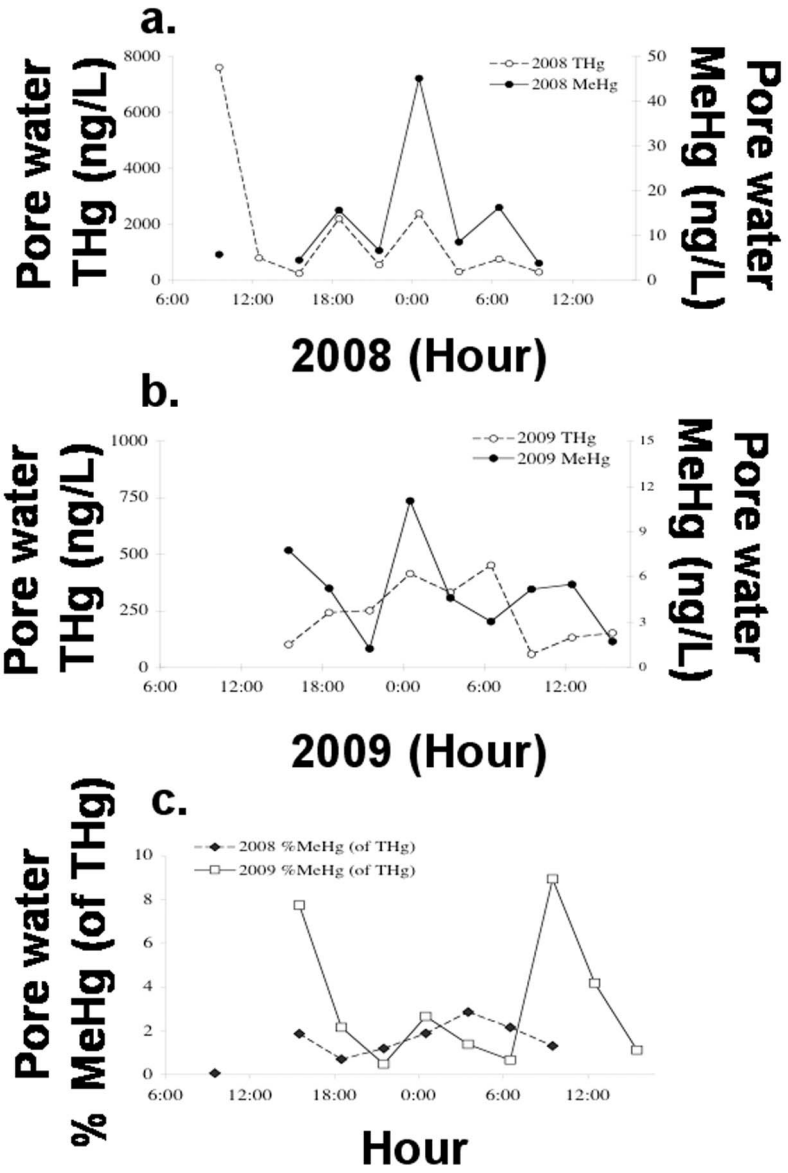

Figure 3. Results for pore water total THg (ng/L) and MeHg (ng/L) (0–2 cm depth) from 24-h sampling in the rice-planted section in (a) 2008 and (b) 2009 and (c) %MeHg (of THg) (unitless) for both years.

date (ANOVA, $p < 0.05$ for both $\log_{10}$-transformed and raw data), except for pore water MeHg levels in fallow section (ANOVA, $p > 0.20$ for both $\log_{10}$-transformed and raw data) (Figure 2f). MeHg levels in the fallow section remained constant throughout the rice-growing season, although corresponding THg levels were significantly higher between sampling events (ANOVA, $p < 0.05$ for both raw and $\log_{10}$-transformed data). Results suggested the rice-planted section was more dynamic than the fallow section. The greatest increases in pore water MeHg levels in the rice-planted section corresponded to grain-filling (2008) and flowering (2009), indicating there was not one single growth stage for rice associated with highest concentrations of pore water MeHg.

3.3. Diel Pore Water MeHg and THg Measurements

[27] In 2008 and 2009 MeHg levels peaked around mid-night before declining, and in 2009 a smaller MeHg peak was observed in the late afternoon (Figures 3a–3b). Percent MeHg (of THg) differed between 2008 and 2009, with a higher ratio during the daytime in 2009, which not observed in 2008 (Figure 3c).

[28] Diel MeHg data from other studies are sparse, but revealing. In lake water with dissolved organic matter, MeHg levels peaked at mid-day, which was attributed to abiotic photoproduction of MeHg [*Siciliano et al.*, 2005]. Using benthic flux chambers in Lavaca Bay, Texas, *Gill et al.* [1999] reported increasing MeHg flux between 7 P.M. and 7 A.M., then a rapid decline, while no net change for inorganic Hg(II) flux was observed for the same time period. Additionally, peak MeHg flux coincided with a release of nutrients (ammonium, silicon, and phosphate) and a decrease in dissolved oxygen, implicating microbial activity in the production and flux of MeHg from pore water [*Gill et al.*, 1999]. In the Florida Everglades water column, diel patterns

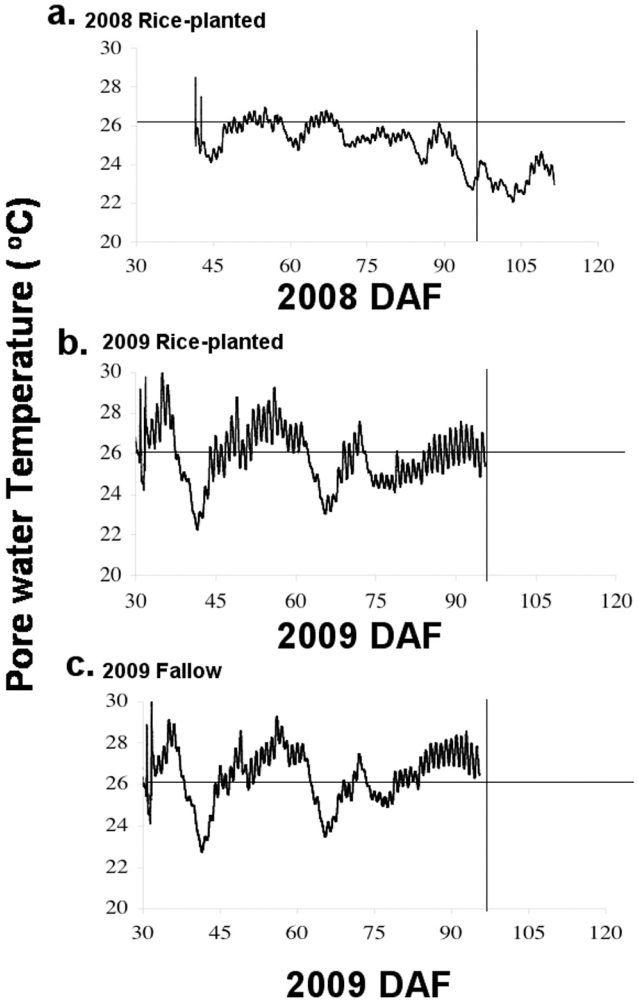

Figure 4. Continuous monitoring of pore water temperature (°C) (in 10-min intervals) versus days after flooding (DAF). The horizontal line represents 26°C and the vertical line represents the date when irrigation was stopped.

were observed for Hg species, including peak concentrations of dissolved gaseous Hg at noon, while net accumulation of MeHg was highest at night [*Krabbenhoft et al.*, 1998]. *Naftz et al.* [2011] reported diurnal cycling in the surface water in wetlands adjacent to the Great Salt Lake (Utah, USA), with lower MeHg concentrations during the day compared to non-daylight periods, suggesting photodegradation was important. In two streams, *Nimick et al.* [2007] observed peak MeHg concentrations during afternoon periods and minimum MeHg concentrations during morning periods, indicating diurnal MeHg cycling in streams was not attributed to photodecomposition. In a tidal wetland, *Bergamaschi et al.* [2011] employed continuous in situ optical measurements of dissolved organic carbon as a proxy for filtered MeHg concentrations, and reported time series data for filtered MeHg alongside other meteorological parameters. Aside from *Gill et al.* [1999], who measured MeHg flux from pore water, other studies addressed diel MeHg cycling in surface water, where photodegradation and/or photoproduction of MeHg were important.

[29] Pore water MeHg levels measured after midnight (at 00:30) in the rice-planted section were 3.4 and 2.2 times higher than average MeHg levels measured during the 24-h period, respectively, while pore water THg levels measured at 00:30 were 1.4 and 1.7 times higher than the average THg levels. In 2009, a second smaller peak was observed in the afternoon at 15:30, when pore water MeHg and THg levels were 1.5 and 0.42 times higher than the mean during the 24-h sampling period. Highest MeHg levels at midnight may reflect decreased competition between SRB and methanogens. Competition between SRB and methanogens is well documented, resulting in lower net Hg(II)-methylation [*Avramescu et al.*, 2011; *Compeau and Bartha*, 1985], although methanogens may promote Hg(II)-methylation in floating microbial mats [*Hamelin et al.*, 2011. Maximum methane emission rates in rice paddies are typically observed in the late afternoon, then declining in the evening [e.g., *Krüger et al.*, 2001], suggesting less competition from methanogens at midnight, the same period when MeHg concentrations were consistently high. However, it is unclear why a second MeHg peak was observed in the late afternoon, when methane emissions were likely highest, and possibly reflected changes in partitioning or MeHg inputs from surface water.

[30] Although processes controlling diel MeHg levels in pore water likely differ from those in surface water (e.g., photodegradation and photomethylation), results from the present study provide additional evidence diurnal cycling of MeHg is important, and field studies may be enhanced by collection of diel MeHg data.

3.4. Pore Water Temperature

[31] In 2008 in the rice-planted section, pore water temperature (±1 sd) averaged 25 ± 1.2°C (range: 22–27°C) and in 2009 averaged 26 ± 1.4°C (range: 22–30°C) in the rice-planted section and 26 ± 1.3°C (range: 23–31°C) in the fallow section (Figure 4). In 2009 at the end of the rice-growing season (>63 DAF), pore water temperature averaged 0.8°C higher in the fallow section compared to the rice-planted section likely due to higher exposure to the sun (i.e., no rice canopy).

3.5. Pore Water pH

[32] In 2008 before irrigation was stopped (i.e.,<96 DAF, before the final ripening stage) and in 2009, pore water pH in the rice-planted section averaged 6.30 and 6.05, respectively, while in 2009 in the fallow section pore water pH averaged 6.95 (Figure 5, Table 3). Following sensor deployment, the rice-planted section quickly became more acidic than the fallow section (Figures 5b–5c). In 2008 sensors were removed 15 days after the paddy was drained, and pH declined in the final 4 days from 6.30 to 5.31 indicating the soil was acidic, likely due to upwind smelting of $HgS_{(s)}$ (see Section 2.1). In 2009 in the fallow section, pH averaged 6.70 between 32 and 62 DAF (between tillering and panicle initiation) and increased to pH 7.19 between 63 and 95 DAF (between panicle initiation and grain filling), reflecting more alkaline conditions at the end of the rice-growing season in the fallow section.

[33] In 2009 higher pore water HCl-extractable Fe(II) concentrations in the rice-planted section compared to the fallow section (Table 3) suggested the source of acidity was not likely Fe(II) oxidation (see equation (1), Introduction).

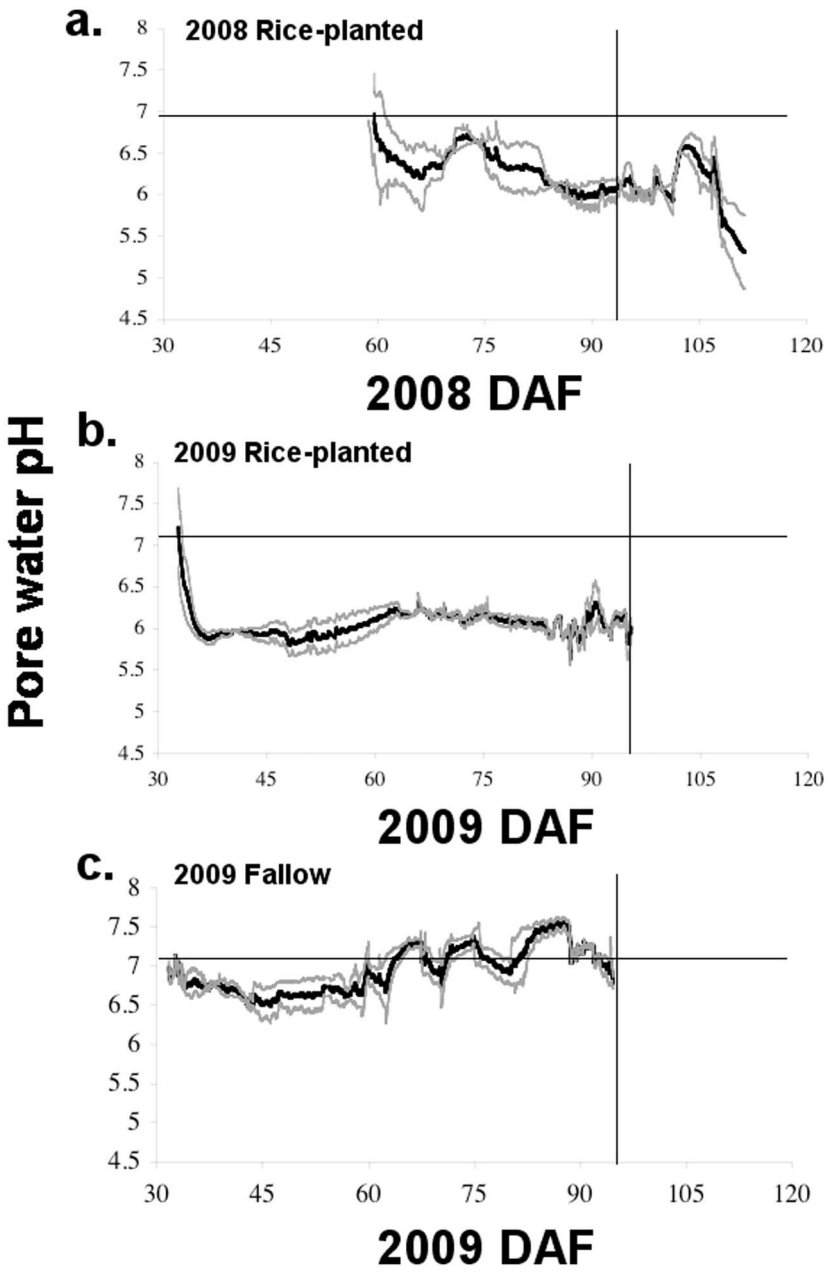

Figure 5. Continuous monitoring of pore water pH (in 10-min intervals) versus days after flooding (DAF), including pH from individual embedded sensors (gray) and the average of each pair of sensors (black). The horizontal line represents pH 7 and the vertical line represents the date when irrigation was stopped.

Instead, lower pH in the rice-planted section possibly reflected the buildup of carbon dioxide (CO_2) due to higher microbial activity. CO_2 buffers the increase in pH and forms H_2CO_3*, which is weak acid (pK_a 6.3), thus lowering pH in the rice-planted section [*Kirk*, 2004]. Lower pH in the rice-planted section may also reflect exudation of protons following uptake of NH_4^+ or release of organic acids from rice roots [*Kirk*, 2004; *Windham-Myers et al.*, 2009]. Results from this study were consistent with *Kostka and Luther* [1995], who reported lower pH and higher pore water Fe (II) concentrations in vegetated sediment compared to non-vegetated sediment in a Fe-rich salt marsh.

3.6. Diel Pore Water pH and Temperature

[34] Diurnal cycling of pore water pH was not observed in both years in both sections of the paddy (Figure 6a). Diurnal cycling of temperature was observed in 2009 but not 2008 (Figure 6b), with minima and maxima temperatures occurring at ~10:00 and 20:00, respectively, which was similar to trends reported by *Krüger et al.* [2001].

[35] Microbial Hg(II)-methylation is a function of both pH and temperature [e.g., *Kelly et al.*, 2003; *Golding et al.*, 2008; *Haitzer et al.*, 2003; *Rothenberg et al.*, 2008; *Ullrich et al.*, 2001]. However, pH and temperature were not likely

Table 3. Results for Pore Water and Sediment Parameters[a]

Matrix	Parameter	2008 Rice-Planted	2009 Rice-Planted	2009 Fallow
Pore water	pH (log-unit)[b]	6.23 (5.31–7.00) [7460]	6.05 (5.63–7.21) [8928]	6.95 (6.49–7.56) [8967]
	Temperature (°C)	25 ± 1.2 (22–28) [10,072]	26 ± 1.4 (22–30) [9483]	26 ± 1.3 (23–31) [9467]
	Sulfate (μM)[c]	61 ± 95 (3.2–330) [24]	100 ± 93 (14–490) [26]	400 ± 670 (12–2100) [25]
	HCl-extractable Fe(II) (μM)	17 ± 10 (3.1–31) [8]	230 ± 170 (5.0–550) [27]	110 ± 120 (5.5–370) [28]
	HCl-extractable FeT (μM)	NA	290 ± 150 (33–640) [28]	190 ± 120 (9.2–390) [27]
	THg (ng/L)[c]	230 ± 190 (9.9–710) [22]	230 ± 200 (22–890) [35]	120 ± 190 (17 − 1000) [33]
	MeHg (ng/L)[c]	4.1 ± 3.7 (0.39–14) [24]	6.3 ± 4.2 (0.79–22) [36]	3.7 ± 1.9 (0.74–8.6) [33]
Sediment	OM (%LOI)	9.3 ± 0.47 (8.5–11) [21]	9.6 ± 0.47 (8.3–11) [32]	9.5 ± 0.45 (8.7–10) [29]
	HCl-extractable Fe(II) (μmol/g)	0.78 ± 0.28 (0.39–1.3) [21]	24 ± 15 (3.1–79) [32]	24 ± 9.8 (9.8–8.8) [41]
	HCl-extractable FeT (μmol/g)	2.1 ± 0.28 (1.5–2.5) [21]	48 ± 20 (16–99) [32]	48 ± 22 (16–100) [29]
	AVS (μmol/g)	NA	0.045 ± 0.064 (0.0014–0.26) [32]	0.052 ± 0.089 (0.00041–0.38) [29]
	THg (μg/g)	8.6 ± 1.4 (5.0–11) [21]	11 ± 0.83 (9.4 − 13) [32]	11 ± 1.2 (9.0–13) [29]
	MeHg (ng/g)	4.5 ± 1.4 (2.6 − 8.0) [21]	3.1 ± 1.4 (0.51 − 6.4) [32]	4.3 ± 2.7 (1.9 − 17) [29]
Log_{10} K_d	THg (L/Kg)[b]	4.6 (4.1–5.2) [19]	4.8 (4.1–5.7) [31]	5.2 (4.1–5.8) [29]
	MeHg (L/Kg)[b]	3.2 (2.4–4.1) [21]	2.7 (2.0–3.2) [32]	3.0 (2.6–3.4) [29]

[a]Parameters include the average ±1 standard deviation (SD) where appropriate; the range, shown in parentheses; and the sample size, shown in brackets. NA indicates that no measurements were taken. The entire data set is available in the auxiliary materials.[1]
[b]Standard deviation not provided for data on a log_{10}-scale.
[c]Includes surface water and pore water.

the main drivers for Hg(II)-methylation in the soil subsurface of the rice-planted section within this 24-h timeframe. A lack of correspondence in diel trends between pH, temperature and MeHg concentrations over a 24-h period suggested biogeochemical controls on MeHg yields differed between short-term (i.e., 24-h) and long-term time scales (i.e., over several weeks).

3.7. Pore Water $(H_2S)_T$ Levels

[36] In 2008, $(H_2S)_T$ levels ranged from 3.7 to 4.1 μM (n = 8 observations) on the first sampling date during panicle initiation (60 DAF), and there was an inverse correspondence between $(H_2S)_T$ and HCl-extractable Fe(II) levels (figure not shown). However, all other $(H_2S)_T$ measurements in 2008 were below the detection level (n = 14 observations).

[37] In 2009, all $(H_2S)_T$ levels measured in pore water extracted from sediment cores were below the detection level (0.10 μM) (rice-planted: n = 26 observations; fallow: n = 24 observations). Corresponding $(H_2S)_T$ values in pore water from peepers, which were preserved under N_2 in the field, were also below the detection level, aside from 1 observation in the rice-planted section (7 cm depth, 54 DAF, 0.74 μM), and 5 observations in the fallow section (7–13 cm depth, 54 and 75 DAF, 0.19–1.1 μM) (figures not shown), indicating the number of non-detects from sediment cores was not an artifact. Peepers deployed on 7 August and retrieved on 27 August (during grain filling) were not analyzed due to dry conditions.

3.8. Surface Water and Pore Water SO_4^{2-} Concentrations

[38] Concentrations of surface water and pore water SO_4^{2-} in the rice-planted section ranged from 3.2 to 330 μM in 2008 (n = 24 observations) and 14–490 μM in 2009 (n = 26 observations), and in 2009 in the fallow section ranged from 12 to 2100 μM (n = 25 observations). Highest SO_4^{2-} levels were observed near the interface between the paddy soil and overlying surface water, then declined with depth (Figure 7). Of the independent parameters measured, pore water SO_4^{2-} and MeHg levels were most correlated in the rice-planted section in 2009 (discussed further in Section 4.1). In 2009 in the fallow section, maximum SO_4^{2-} levels were measured on 28 August (i.e., 95 DAF, 2100 μM) after this section completely dried and was re-irrigated (Figure 7d) (discussed further in Section 4.2).

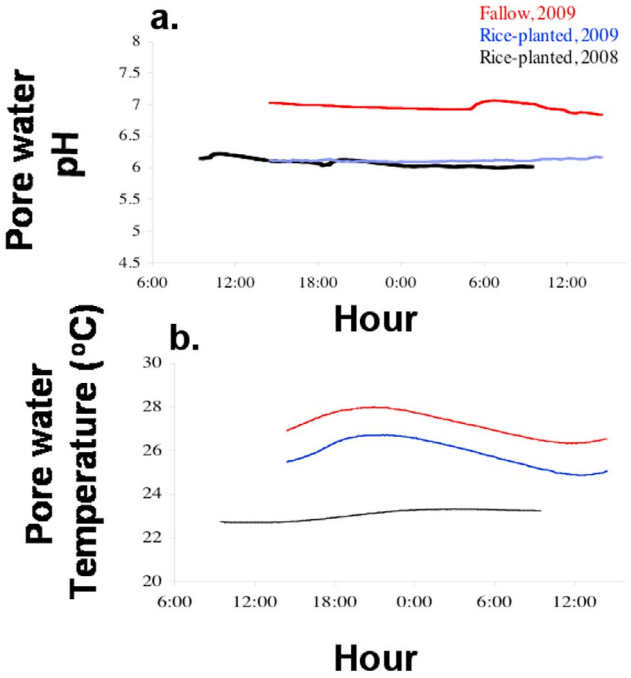

Figure 6. Corresponding measurements during 24-h sampling for (a) pore water pH and (b) pore water temperature (°C). Ten-day average pH and temperature trends for both years were similar (not shown).

[1]Auxiliary materials are available at ftp://ftp.agu.org/apend/jg/2011JG001800.

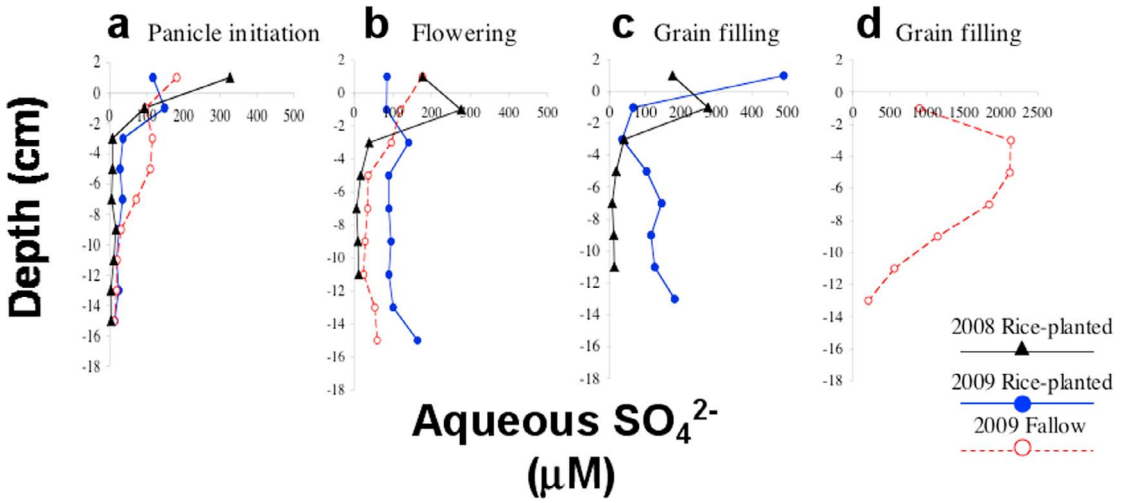

Figure 7. Surface water and pore water sulfate (SO_4^{2-}) concentrations (μM).

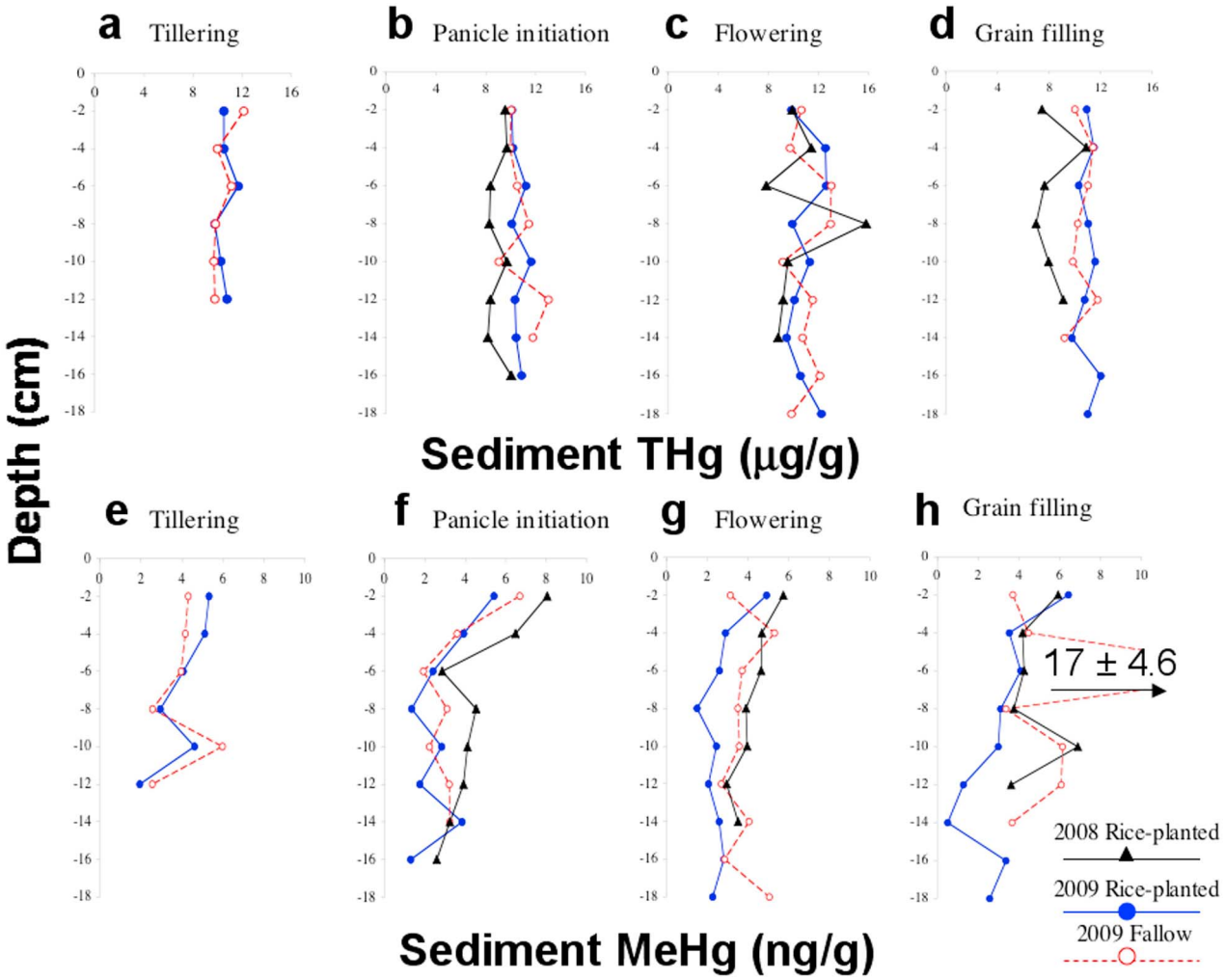

Figure 8. Depth profiles of sediment concentrations of THg (μg/g) (a–d) and MeHg (ng/g) (e–h).

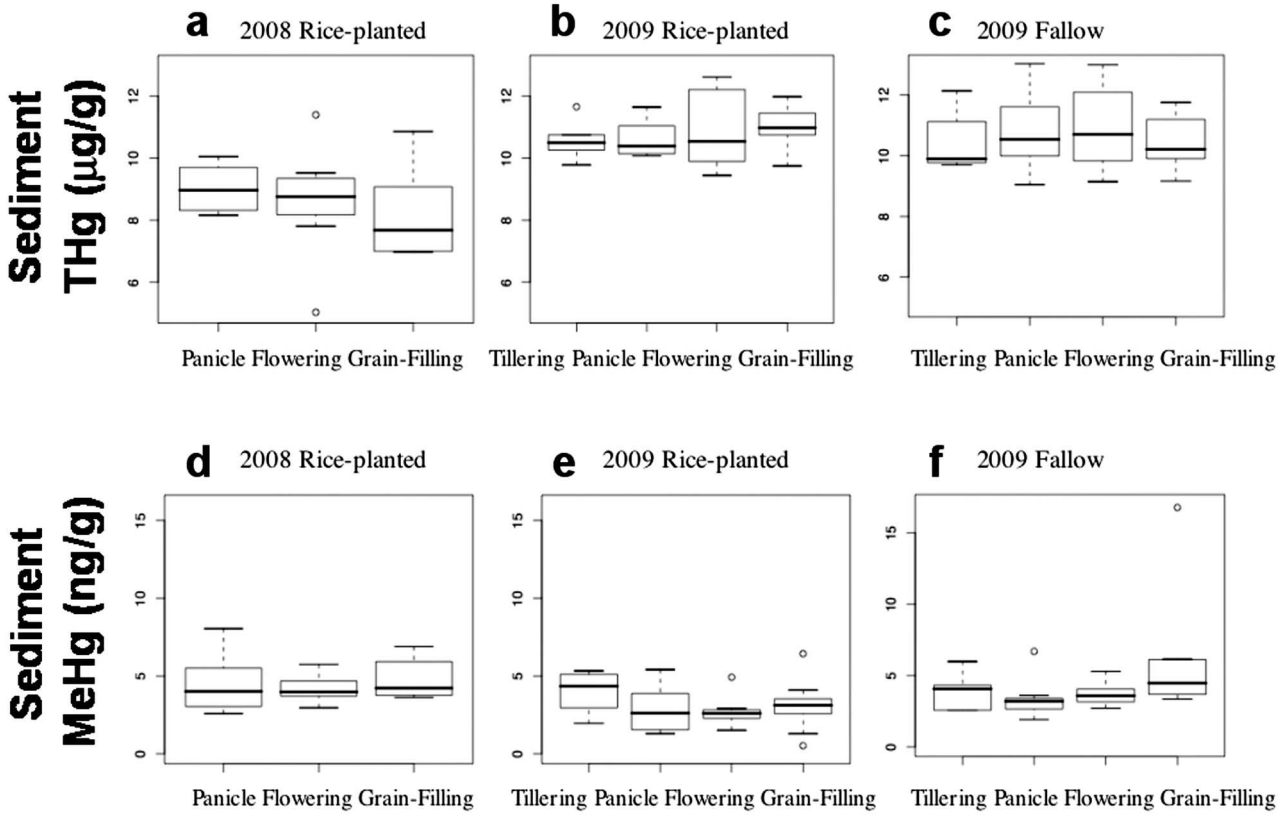

Figure 9. Boxplots for sediment concentrations of THg (μg/g) (a–c) and MeHg (ng/g) (d–f) aggregated for each time point when samples were collected (i.e., tillering, panicle initiation, flowering and grain-filling). There were no significant differences between time points within each boxplot (ANOVA, $p > 0.05$).

3.9. Partitioning of THg and MeHg

[39] Partitioning coefficients (K_d, L/Kg) for THg and MeHg were calculated as follows:

$$K_d = \frac{[Hg_{sed}]}{[Hg_{pw}]} \times 1000 \quad (2)$$

where $[Hg_{sed}]$ and $[Hg_{pw}]$ were the concentrations of THg or MeHg in sediment (ng/g) or pore water (ng/L), respectively, and results were reported after $\log_{10}$-transformation (Table 3). Complexation of metals varies according to pH, ionic strength of the solution, organic ligands, and other factors [*McBride*, 1994]. In both years and in both sections of the rice paddy, observations for K_d THg were greater than K_d MeHg (paired t-test, $p < 0.001$ for all 3 models), which was consistent with other studies concerning Hg cycling and partitioning at the sediment-water interface (e.g., *Hammerschmidt and Fitzgerald*, 2004; *Hammerschmidt et al.*, 2008; *Hollweg et al.*, 2010; *Muresan et al.*, 2007; *Rothenberg et al.*, 2008]. Differences possibly reflected size and/or charge differences between inorganic Hg(II) and MeHg species. In 2009 K_d values for THg and MeHg were significantly higher in the fallow section compared to the rice-planted section in 2009 (paired t-tests, $p < 0.001$ for both models), where average pH was also up to 1 log-unit higher (see Section 3.4). Lower K_d THg levels in the rice-planted section (Table 3) indicated greater dissolution of THg (i.e., higher bioavailability) at lower pH, which was consistent with other reports [*Haitzer et al.*, 2003].

3.10. Sediment THg and MeHg Levels

[40] In 2008 and 2009 in the rice-planted section, sediment MeHg levels averaged 4.5 $\pm$ 1.4 ng/g (n = 21 observations) and 3.1 $\pm$ 1.4 ng/g (n = 32 observations), respectively, and in 2009 in the fallow section sediment MeHg levels averaged 4.3 $\pm$ 2.7 ng/g (n = 29 observations) (Figure 8). Sediment MeHg concentrations in the rice-planted section in 2008 were significantly higher than the rice-planted section in 2009 (ANOVA, $p < 0.05$ for both $\log_{10}$-transformed and raw data). Unlike pore water THg and MeHg concentrations (Section 3.2, Figure 2), sediment THg and MeHg concentrations did not change throughout the rice-growing season (Figure 9) (ANOVA, $p > 0.10$ for all analyses when raw and $\log_{10}$-transformed data). Percent MeHg (of THg) averaged < 0.1% under all three scenarios, and sediment MeHg and THg levels were uncorrelated (for all three regressions, $r^2 < 0.02$, $p > 0.50$, when both variables were $\log_{10}$-transformed and when using raw data). The latter result differed from *Benoit et al.* [2003], who combined data from 25 sites and reported a positive linear relationship between sediment MeHg and THg levels ($r^2 = 0.40$, both variables $\log_{10}$-transformed), and may reflect differences in scale (THg: 1–10^6 ng/g; MeHg:

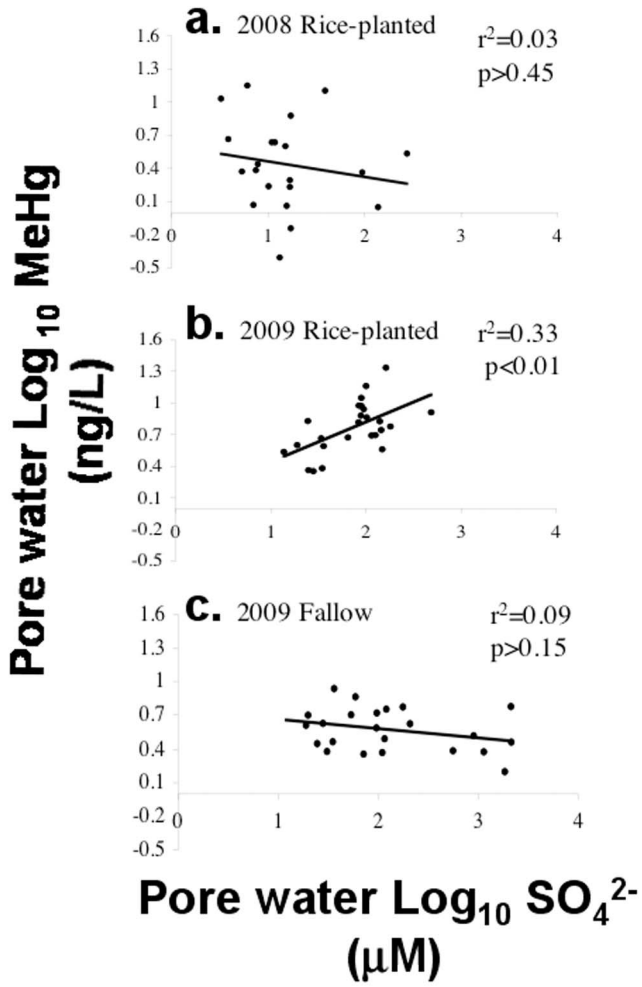

Figure 10. Scatterplots for pore water MeHg (ng/L) versus sulfate (SO_4^{2-}) (μM).

0.01–100 ng/g, from *Benoit et al.* [2003]; THg: 5000–13 000 ng/g; MeHg: 0.51–17 ng/g, from this study).

4. Discussion

4.1. Pore Water MeHg Concentrations and Cycling of Fe and Sulfur (S)

[41] In 2009 in the rice-planted section, pore water MeHg and SO_4^{2-} levels were positively correlated (r^2 = 0.33, $p < 0.01$, when both variables were $\log_{10}$-transformed; r^2 = 0.088, $p > 0.10$ when using raw data), but the same parameters were weakly correlated in 2008 in the rice-planted section and in 2009 in the fallow section ($r^2 < 0.09$, $p > 0.15$ for both regressions when both variables $\log_{10}$-transformed and using raw data) (Figure 10). All other independent parameters measured in pore water and sediment, including pore water HCl-extractable Fe(II) concentrations, were less correlated with pore water MeHg concentrations (figures not shown).

[42] Researchers report the distribution between Hg(II) methylation rates and SO_4^{2-} levels hypothetically resembles a bell-shaped curve (i.e., not linear), with peak MeHg yields between 200 and 500 μM SO_4^{2-} [*Gilmour and Henry*, 1991; *Gilmour et al.*, 1998; *Muresan et al.*, 2007; *Orem et al.*, 2011]. When SO_4^{2-} is low (i.e.,<200 μM), SO_4^{2-} reduction rates are limited and hence MeHg yields are lower, while at higher SO_4^{2-} levels (i.e.,>500 μM), $(H_2S)_T$ levels are higher and the fraction of more bioavailable $HgS^o_{(aq)}$ decreases, lowering predicted Hg methylation rates [*Gilmour and Henry*, 1991]. In both years and in the rice-planted and fallow sections, SO_4^{2-} levels were <200 μM (=86th percentile) and $(H_2S)_T$ levels were <10 μM, yet a positive correlation between MeHg and SO_4^{2-} levels was observed only in 2009 in the rice-planted section. Differences between years and between sites may reflect a link between Hg(II)-methylation and Fe and S cycling. In 2009 sediment HCl-extractable Fe(II) and FeT levels were 20–30 times higher compared to 2008 (Table 3). Higher Fe inputs in 2009 in both the rice-planted and fallow sections were possibly due to upwind smelting of Fe-containing Hg minerals or waste in artisanal smelters (see Section 2.1), which were occasionally active during the summer, or possibly due to fertilizer applications containing Fe.

[43] Fe cycling may impact Hg(II)-methylation in several ways. FeRB directly methylate Hg [*Fleming et al.*, 2006; *Kerin et al.*, 2006], which was reported for a salt marsh where Fe(III) reduction was the dominant microbial process [*Mitchell and Gilmour*, 2008]. Fe cycling may increase the solubility of Hg(II) via oxidation of S(-II) by Fe(III), which forms S(0) and polysulfides and may cause the dissolution of inorganic Hg(II) [*Slowey and Brown*, 2007]. Production of amorphous Fe(III) was associated with higher MeHg production in several wetland sites, including rice paddies [*Windham-Myers et al.*, 2009]. *Yu et al.* [2012] reported increased potential Hg(II)-methylation rates when freshwater lake sediment was spiked with sulfate and amorphous Fe(III) oxyhydroxide, and suggested both SRB and FeRB contributed to Hg(II)-methylation. In rice paddies, 20–80% of Fe is present as Fe(III)-oxides and up to 90% is reduced to soluble Fe(II) following flooding, which may be precipitated as $FeS_{(s)}$ or Fe(II)/Fe(III) compounds [*Kirk*, 2004]. By binding S(-II), $FeS_{(s)}$ may increase the bioavailability of $HgS^o_{(aq)}$ and thus increase MeHg yields [*Benoit et al.*, 1999, 2001], or when sediment Fe(II) levels are higher, $FeS_{(s)}$ may sorb dissolved inorganic Hg(II), thus decreasing available substrate and lowering Hg(II)-methylation rates [*Mehrotra et al.*, 2003; *Mehrotra and Sedlak*, 2005; *Ulrich and Sedlak*, 2010].

[44] For this study, the precipitation of $FeS_{(s)}$ was estimated using average pore water HCl-extractable Fe(II) levels (as $[Fe\bullet II]_T$) (Table 3), the detection level for $(H_2S)_T$ (0.10 μM) (as $[S\bullet\text{-}II]_T$), and the following equations, including (3) when no $FeS_{(s)}$ precipitates, which may be simplified at low pH to $[Fe\bullet II] = [Fe^{2+}]$, and (4) when $FeS_{(s)}$ forms [*Morel and Hering*, 1993] (see Table 4):

$$[Fe^{2+}] = \frac{[Fe \cdot II]_T}{1 + \frac{10^{-9.5}}{[H^+]} + \frac{10^{-20.6}}{[H^+]^2} + \frac{10^{-31}}{[H^+]^3}} \quad (3)$$

$$[Fe^{2+}] = \frac{K_{s1}}{[S^{2-}]} = \frac{10^{-18.1}}{[S^{2-}]} = \frac{10^{-18.1}}{[S \cdot -II]_T\left(\left(10^{20.9}[H^+]^2 + 10^{13.9}[H^+]\right)^{-1}\right)} \quad (4)$$

Table 4. Reactions to Predict Formation of $FeS_{(s)}$ and Disassociation Constants (pK) [*Morel and Hering*, 1993]

$H_2O = H^+ + OH^-$	$pK_w = 14$
$H_2S = HS - + H^+$	pK = 7.0
$HS^- = S(-II) + H^+$	pK = 13.9
$H_2CO_3^* = HCO_3^- + H^+$	pK = 6.3
$HCO_3^- = CO_3^{2-} + H^+$	pK = 10.3
$FeS(s) = Fe(II) + S(-II)$	$pK_{s1} = 18.1$
$FeCO_3(s) + 2\ H^+ = Fe(II) + 2H_2O$	$pK_{s2} = 10.7$
$Fe(OH)_2(s) + 2\ H^+ = Fe(II) + 2H_2O$	$pK_{s3} = -12.9$
$FeOH^+ + H^+ = Fe(II) + H_2O$	pK = −9.5
$Fe(OH)_2^0 + 2\ H^+ = Fe(II) + 2\ H_2O$	pK = −20.6
$Fe(OH)_3^- + 3\ H^+ = Fe(II) + 2\ H_2O$	pK = −31.0

To estimate formation of $FeS_{(s)}$ reactions (3) and (4) were equated, and critical pH values were determined [*Morel and Hering*, 1993], including pH 7.66 (in 2008 in the rice-planted section), pH 6.83 (in 2009 in the rice-planted section) and pH 7.04 (in 2009 in the fallow section). Using pH data collected in 10-min intervals throughout both rice-growing seasons (Section 3.4, Figure 5), $FeS_{(s)}$ was unlikely to form in both years in the rice-planted section because the critical pH values were between the 99th and 100th percentiles, while in 2009 in the fallow section the critical pH value was in the 60th percentile, indicating $FeS_{(s)}$ was a sink for S(-II) in the fallow section but not in the rice-planted section.

[45] In anoxic sediment, Fe and S cycling are linked abiotically as follows [*Rickard and Luther*, 2007]:

$$Fe(III) + H_2S \rightarrow Fe(II) + S_8 + S_n^{2-} \quad (5)$$

$$Fe(II) + H_2S \rightarrow FeS + 2H^+ \quad (6)$$

$$FeS + S_8/S_n^{2-} \rightarrow FeS_2 + S_{n-1}^{2-} \quad (7)$$

$$FeS + H_2S \rightarrow FeS_2 + H_2 \quad (8)$$

However, the transition from Fe(II) to $FeS_{(s)}$ may be disrupted by processes bringing O_2 or nitrate (NO_3^-) at depth, including burrowing of organisms (i.e., bioturbation) and growth of plants [*Rickard and Luther*, 2007]. In rice paddies, O_2 is leaked from rice roots into the rhizosphere through aerenchyma [*Colmer*, 2003] (see Introduction), possibly preventing the formation of $FeS_{(s)}$. In 2009 in the rice-planted section, most $(H_2S)_T$ values were below the detection level (Section 3.6), yet MeHg and SO_4^{2-} concentrations were positively correlated. Instead of forming $FeS_{(s)}$, it is hypothesized that Fe(III) oxidized excess S(-II), and then intermediate S species, including polysulfides and S(0), were further oxidized to SO_4^{2-}, thus prolonging SO_4^{2-} reduction in the rice-planted section and increasing Hg(II)-methylation. Under these conditions, Fe(III) may also be re-formed, replenishing electron acceptors for both FeRB and SRB. This hypothesis is consistent with results from *Kostka and Luther* [1995], who reported plant roots provided oxidation and organic matter in vegetated sediment, where reactive Fe(III) cycling was governed by SO_4^{2-} cycling, which was not observed in unvegetated sediment.

[46] It may be useful to consider the ratio between concentrations of pore water SO_4^{2-} and sediment HCl-extractable Fe (III). *Lovley and Phillips* [1987a] reported FeRB outcompeted SRB due to a lower threshold for electron donors, using concentrations of pore water SO_4^{2-} (=3100 μM) and sediment Fe(III) (=50 μmol/g), i.e., the ratio between both parameters was 62 g/L. For this study, the ratio for the same parameters was as follows: 2009 rice-planted 6.8 ± 9.0 g/L (with one observation deleted, when sediment Fe(III) was ~0 μmol/g); 2008 rice-planted 26 ± 45 g/L; 2009 fallow 57 ± 120 g/L), with a significantly lower ratio in 2009 in the rice-planted section (ANOVA, $p < 0.01$ when data were $\log_{10}$-transformed, $p > 0.15$ using raw data). When this ratio is higher, there may be insufficient Fe(III) to oxidize excess S(-II) and SO_4^{2-} reduction may decrease, while a lower ratio (observed in 2009 in the rice-planted section) may reflect conditions conducive for both FeRB and SRB.

4.2. The Impact of Alternating Wetting and Drying on Sediment MeHg Concentrations

[47] Peak sediment MeHg levels were observed in 2009 in the fallow section, and this was the largest increase in sediment MeHg levels during the rice-growing season (Figure 8h). Between June and August 36% less rain fell compared to 2008 (2008: 506 mm, 2009: 325 mm), including no precipitation between 7 August and 27 August (corresponding to 75 and 94 DAF, between flowering and grain filling) (Junfang Zhang, Guizhou Institute of Environmental Science and Design, personal communication). The rice-planted section was protected by the rice canopy and remained saturated, while the fallow section dried. A few hours after the paddy was re-irrigated on 27 August, sediment cores were collected for this analysis. In the fallow section at 5 cm depth, peak concentrations of sediment MeHg and pore water SO_4^{2-} levels were 4.6 and 2.5 standard deviations above the mean, respectively, while the same parameters were 0.72 and −0.73 standard deviations from the mean in the rice-planted section. Pore water Fe(II) levels in the fallow and rice-planted section were −0.55 and 0.99 standard deviations from the mean, respectively. One explanation is that flooding of the dried paddy soil in the fallow section caused a pulse in Hg(II)-methylation following stimulation of SRB, then quick resorption of MeHg to sediment.

[48] Alternating wetting and drying is one approach employed throughout Asia to reduce freshwater use for rice production [*Bouman et al.*, 2007; *Dong et al.*, 2004; *Rothenberg et al.*, 2011]. Results from the present study indicate water-saving rice cultivation practices may increase Hg(II)-methylation if the paddy is allowed to completely dry and then re-wetted. Previous research indicated concentrations of paddy soil MeHg and rice grain MeHg were positively correlated [e.g., *Rothenberg et al.*, 2011]. More research is needed to optimize irrigation methods to mitigate exposure to MeHg through rice ingestion.

5. Conclusions

[49] Given the importance of rice paddies for global food consumption, it is vital to investigate processes controlling Hg cycling in flooded rice fields. Results indicated the rice-planted section was on average more acidic than the fallow section, and therefore not a sink for $FeS_{(s)}$. Instead of forming $FeS_{(s)}$, it is hypothesized Fe(III) oxidized excess S(-II), producing intermediate S species, which were oxidized to SO_4^{2-}, replenishing electron acceptors for SRB and promoting Hg

(II)-methylation. Results suggest Fe(III) reduction indirectly enhanced Hg(II)-methylation. Although O_2 leakage from rice roots may directly oxidize S(-II), results from both 2008 and 2009 indicated a balance between concentrations of pore water SO_4^{2-} and sediment Fe(III) was also important, and should be further investigated.

[50] Sediment MeHg levels spiked after the fallow section of the paddy was completely dried and re-wetted. Rice farmers in Asia are under pressure to reduce consumption of freshwater resources for rice cultivation, including implementation of alternating wetting and drying; however, results indicated more research is required to optimize irrigation methods to mitigate (not promote) MeHg production in rice paddies, which may be translocated from paddy soil to rice grain.

[51] **Acknowledgments.** The authors wish to thank Liu Jinling, Liu Na, and Yuan Xiaobo for laboratory and field assistance and the anonymous reviewers who provided thorough comments, which greatly enhanced the interpretation of the data. S.E.R. was supported by the U.S. National Science Foundation International Research Development Program (grant 0802014), X.F. was funded by the Natural Science Foundation of China (grant 41021062), and both authors were supported by the Institute of Geochemistry, State Key Laboratory of Environmental Geochemistry, Chinese Academy of Sciences, in Guiyang, China.

References

Achtnich, C., F. Bak, and R. Conrad (1995), Competition for electron donors among nitrate reducers, ferric iron reducers, sulfate reducers, and methanogens in anoxic paddy soil, *Biol. Fertil. Soils*, *19*, 65–72, doi:10.1007/BF00336349.

Allen, H. E., G. Fu, and B. Deng (1993), Analysis of acid-volatile sulfide (AVS) and simultaneously extracted metals (SEM) for the estimation of potential toxicity in aquatic sediments, *Environ. Toxicol. Chem.*, *12*, 1441–1453, doi:10.1002/etc.5620120812.

Avramescu, M.-L., E. Yumvihoze, H. Hintelmann, J. Ridal, D. Fortin, and D. R. S. Lean (2011), Biogeochemical factors influencing net mercury methylation in contaminated freshwater sediments from the St. Lawrence River in Cornwell, Ontario, Canada, *Sci. Total Environ.*, *409*, 968–978, doi:10.1016/j.scitotenv.2010.11.016.

Begg, C. B. M., G. J. D. Kirk, A. F. Mackenzie, and H. U. Neue (1994), Root-induced iron oxidation and pH changes in the lowland rice rhizosphere, *New Phytol.*, *128*, 469–477, doi:10.1111/j.1469-8137.1994.tb02993.x.

Benoit, J. M., C. C. Gilmour, R. P. Mason, and A. Heyes (1999), Sulfide controls on mercury speciation and bioavailability to methylating bacteria in sediment pore waters, *Environ. Sci. Technol.*, *33*, 951–957, doi:10.1021/es9808200.

Benoit, J. M., C. C. Gilmour, and R. P. Mason (2001), The influence of sulfide on solid-phase mercury bioavailability for methylation by pure cultures of *Desulfobulbus propionicus* (1pr3), *Environ. Sci. Technol.*, *35*, 127–132, doi:10.1021/es001415n.

Benoit, J. M., C. C. Gilmour, A. Heyes, R. P. Mason, and C. L. Miller (2003), Geochemical and biological controls over methylmercury production and degradation in aquatic ecosystems, in *Biogeochemistry of Environmentally Important Trace Elements*, *ACS Symposium Ser. 835*, edited by Y. Cai and O. C. Braids, pp. 262–297, Am. Chem. Soc., Washington, D. C.

Bergamaschi, B. A., et al. (2011), Methyl mercury dynamics in a tidal wetland quantified using in situ optical measurements, *Limnol. Oceanogr.*, *56*, 1355–1371, doi:10.4319/lo.2011.56.4.1355.

Bloom, N. S., C. J. Watras, and J. P. Hurley (1991), Impact of acidification on the methylmercury cycle of remote seepage lakes, *Water Air Soil Pollut.*, *56*, 477–491, doi:10.1007/BF00342293.

Bouman, B. A. M., R. M. Lampayan, and T. P. Tuong (Eds.) (2007), *Water Management in Irrigated Rice: Coping with Water Scarcity*, Int. Rice Res. Inst., Los Baños, Philippines.

Cline, J. D. (1969), Spectrophotometric determination of hydrogen sulfide in natural waters, *Limnol. Oceanogr.*, *14*, 454–458, doi:10.4319/lo.1969.14.3.0454.

Colmer, T. (2003), Long-distance transport of gases in plants: A perspective on internal aeration and radial oxygen loss from roots, *Plant Cell Environ.*, *26*, 17–36, doi:10.1046/j.1365-3040.2003.00846.x.

Compeau, G. C., and R. Bartha (1985), Sulfate-reducing bacteria: Principal methylators of mercury in anoxic estuarine sediment, *Appl. Environ. Microbiol.*, *50*, 498–502.

Dong, B., D. Molden, R. Loeve, Y. H. Li, C. D. Chen, and J. Z. Wang (2004), Farm level practices and water productivity in Zhanghe Irrigation System, *Paddy Water Environ.*, *2*, 217–226, doi:10.1007/s10333-004-0066-z.

Fairhurst, T., C. Witt, R. Buresh, and A. Dobermann (Eds.) (2007), *Rice: A Practical Guide to Nutrient Management*, 2nd ed., Int. Rice Res. Inst., Los Baños, Philippines.

Feng, X., et al. (2008), Human exposure to methylmercury through rice intake in mercury mining areas, Guizhou province, China, *Environ. Sci. Technol.*, *42*, 326–332, doi:10.1021/es071948x.

Fleming, E. J., E. E. Mack, P. G. Green, and D. C. Nelson (2006), Mercury methylation from unexpected sources: Molybdate-inhibited freshwater sediments and an iron-reducing bacterium, *Appl. Environ. Microbiol.*, *72*, 457–464, doi:10.1128/AEM.72.1.457-464.2006.

Gibbs, M. M. (1979), Simple method for the rapid determination of iron in natural waters, *Water Res.*, *13*, 295–297, doi:10.1016/0043-1354(79)90209-4.

Gill, G. A., N. S. Bloom, S. Cappellino, C. T. Driscoll, C. Dobbs, L. McShea, R. P. Mason, and J. W. M. Rudd (1999), Sediment-water fluxes of mercury in Lavaca Bay, Texas, *Environ. Sci. Technol.*, *33*, 663–669, doi:10.1021/es980380c.

Gilmour, C. C., and E. A. Henry (1991), Mercury methylation in aquatic systems affected by acid deposition, *Environ. Pollut.*, *71*, 131–169, doi:10.1016/0269-7491(91)90031-Q.

Gilmour, C. C., E. A. Henry, and R. Mitchell (1992), Sulfate stimulation of mercury methylation in freshwater sediments, *Environ. Sci. Technol.*, *26*, 2281–2287, doi:10.1021/es00035a029.

Gilmour, C. C., G. S. Riedel, M. C. Ederington, J. T. Bell, J. M. Benoit, G. A. Gill, and M. C. Stordal (1998), Methylmercury concentrations and production rates across a trophic gradient in the northern Everglades, *Biogeochemistry*, *40*, 327–345, doi:10.1023/A:1005972708616.

Golding, G. R., R. Sparling, and C. A. Kelly (2008), Effect of pH on intracellular accumulation of trace concentrations of Hg(II) in Escerichia coli under anaerobic conditions, as measured using a mer-lux bioreporter, *Appl. Environ. Microbiol.*, *74*, 667–675, doi:10.1128/AEM.00717-07.

Haitzer, M., G. R. Aiken, and J. N. Ryan (2003), Binding of mercury(II) to aquatic humic substances: Influence of pH and source of humic substances, *Environ. Sci. Technol.*, *37*, 2436–2441, doi:10.1021/es026291o.

Hamelin, S., M. Amyot, T. Barkay, Y. Wang, and D. Planas (2011), Methanogens: Principal methylators of mercury in lake periphyton, *Environ. Sci. Technol.*, *45*, 7693–7700, dx.doi.org/10.1021/es2010072, doi:10.1021/es2010072.

Hammerschmidt, C. R., and W. F. Fitzgerald (2004), Geochemical controls on the production and distribution of methylmercury in near-shore marine sediments, *Environ. Sci. Technol.*, *38*, 1487–1495, doi:10.1021/es034528q.

Hammerschmidt, C. R., W. F. Fitzgerald, P. H. Balcom, and P. T. Visscher (2008), Organic matter and sulfide inhibit methylmercury production in sediments of New York/New Jersey Harbor, *Mar. Chem.*, *109*, 165–182, doi:10.1016/j.marchem.2008.01.007.

Hollweg, T. A., C. C. Gilmour, and R. P. Mason (2010), Mercury and methylmercury cycling in sediments of the mid-Atlantic continental shelf and slope, *Limnol. Oceanogr.*, *55*, 2703–2722, doi:10.4319/lo.2010.55.6.2703.

Horvat, M., et al. (2003), Total mercury, methylmercury and selenium in mercury polluted areas in the province Guizhou, China, *Sci. Total Environ.*, *304*, 231–256, doi:10.1016/S0048-9697(02)00572-7.

Kelly, C. A., J. W. M. Rudd, and M. H. Holoka (2003), Effect of pH on mercury uptake by an aquatic bacterium: Implications for Hg cycling, *Environ. Sci. Technol.*, *37*, 2941–2946, doi:10.1021/es026366o.

Kerin, E. J., C. C. Gilmour, E. Roden, M. T. Suzuki, J. D. Coates, and R. P. Mason (2006), Mercury methylation by dissimilatory iron-reducing bacteria, *Appl. Environ. Microbiol.*, *72*, 7919–7921, doi:10.1128/AEM.01602-06.

Kirk, G. (2004), *The Biogeochemistry of Submerged Soils*, John Wiley, West Sussex, U. K., doi:10.1002/047086303X.

Kostka, J. E., and G. W. Luther (1995), Seasonal cycling of Fe in saltmarsh sediments, *Biogeochemistry*, *29*, 159–181, doi:10.1007/BF00000230.

Krabbenhoft, D. P., J. P. Hurley, M. L. Olson, and L. B. Cleckner (1998), Diel variability of mercury phase and species distributions in the Florida Everglades, *Biogeochemistry*, *40*, 311–325, doi:10.1023/A:1005938607225.

Krüger, M., P. Frenzel, and R. Conrad (2001), Microbial processes influencing methane emission from rice fields, *Global Change Biol.*, *7*, 49–63, doi:10.1046/j.1365-2486.2001.00395.x.

Li, P., X. Feng, G. Qiu, L. Shang, S. Wang, and B. Meng (2009), Atmospheric mercury emission from artisanal mercury mining in Guizhou

Province, Southwestern China, *Atmos. Environ.*, *43*, 2247–2251, doi:10.1016/j.atmosenv.2009.01.050.

Liang, L., M. Horvat, X. Feng, L. Shang, H. Li, and P. Pang (2004), Re-evaluation of distillation and comparison with HNO_3 leaching/solvent extraction for isolation of methylmercury compounds from sediment/soil samples, *Appl. Organometal. Chem.*, *18*, 264–270, doi:10.1002/aoc.617.

Lovley, D. R., and E. J. P. Phillips (1987a), Competitive mechanisms for inhibition of sulfate reduction and methane production in the zone of ferric iron reduction in sediments, *Appl. Environ. Microbiol.*, *53*, 2636–2641.

Lovley, D. R., and E. J. P. Phillips (1987b), Rapid assay for microbially reducible ferric iron in aquatic sediments, *Appl. Environ. Microbiol.*, *53*, 1536–1540.

McBride, M. B. (1994), *Environmental Chemistry of Soils*, Oxford Univ. Press, New York, USA.

Mehrotra, A. S., and D. L. Sedlak (2005), Decrease in net mercury methylation rates following iron amendment to anoxic wetland sediment slurries, *Environ. Sci. Technol.*, *39*, 2564–2570, doi:10.1021/es049096d.

Mehrotra, A., A. J. Horne, and D. L. Sedlak (2003), Reduction of net mercury methylation by iron in Desulfobulbus propionicus (1pr3) cultures: Implications for engineered wetlands, *Environ. Sci. Technol.*, *37*, 3018–3023, doi:10.1021/es0262838.

Mitchell, C. P. J., and C. C. Gilmour (2008), Methylmercury production in a Chesapeake Bay salt marsh, *J. Geophys. Res.*, *113*, G00C04, doi:10.1029/2008JG000765.

Morel, F. M. M., and J. G. Hering (1993), *Principles and Applications of Aquatic Chemistry*, John Wiley, New York.

Muresan, B., D. Cossa, D. Jézéquel, F. Prévot, and S. Kerbellec (2007), The biogeochemistry of mercury at the sediment-water interface in the Thao lagoon. 1. Partition and speciation, *Estuarine Coastal Shelf Sci.*, *72*, 472–484, doi:10.1016/j.ecss.2006.11.015.

Naftz, D. L., J. R. Cederberg, D. P. Krabbenhoft, K. R. Beisner, J. Whitehead, and J. Gardberg (2011), Diurnal trends in methylmercury concentration in a wetland adjacent to Great Salt Lake, Utah, USA, *Chem. Geol.*, *283*, 78–86, doi:10.1016/j.chemgeo.2011.02.005.

Nimick, D. A., B. R. McCleskey, C. H. Gammons, T. E. Cleasby, and S. R. Parker (2007), Diel mercury-concentration variations in streams affected by mining and geothermal discharge, *Sci. Total Environ.*, *373*, 344–355, doi:10.1016/j.scitotenv.2006.11.008.

Orem, W., C. C. Gilmour, D. Axelrad, D. Krabbenhoft, D. Scheidt, P. Kalla, P. McCormick, M. Gabriel, and G. Aiken (2011), Sulfur in the South Florida ecosystem: Distribution, sources, biogeochemistry, impacts, and management for restoration, *Crit. Rev. Environ. Sci. Technol.*, *41*(Suppl.), 249–288, doi:10.1080/10643389.2010.531201.

Pacyna, E. G., J. M. Pacyna, K. Sundseth, J. Munthe, K. Kindbom, S. Wilson, F. Steenhuisen, and P. Maxson (2010), Global emission of mercury to the atmosphere from anthropogenic sources in 2005 and projections to 2020, *Atmos. Environ.*, *44*, 2487–2499, doi:10.1016/j.atmosenv.2009.06.009.

Rickard, D., and G. W. Luther III (2007), Chemistry of iron sulfides, *Chem. Rev.*, *107*, 514–562, doi:10.1021/cr0503658.

Rothenberg, S. E., R. F. Ambrose, and J. A. Jay (2008), Mercury cycling in surface water, pore water and sediments of Mugu Lagoon, CA, USA, *Environ. Pollut.*, *154*, 32–45, doi:10.1016/j.envpol.2007.12.013.

Rothenberg, S. E., M. E. Kirby, B. W. Bird, M. B. DeRose, C.-C. Lin, X. Feng, R. F. Ambrose, and J. A. Jay (2010), The impact of over 100 years of wildfires on mercury levels and accumulation rates in two lakes in southern California, USA, *Environ. Earth Sci.*, *60*, 993–1005, doi:10.1007/s12665-009-0238-7.

Rothenberg, S. E., X. Feng, B. Dong, L. Shang, R. Yin, and X. Yuan (2011), Characterization of mercury species in brown and white rice (*Oryza sativa* L.) grown in water-saving paddies, *Environ. Pollut.*, *159*, 1283–1289, doi:10.1016/j.envpol.2011.01.027.

Rothenberg, S. E., X. Feng, W. Zhou, M. Tu, B. Jin, and J. You (2012), Environment and genotype controls on mercury accumulation in rice (*Oryza sativa* L.) cultivated along a contamination gradient in Guizhou, China, *Sci. Total Environ.*, *426*, 272–280, doi:10.1016/j.scitotenv.2012.03.024.

Scheid, D., S. Stubner, and R. Conrad (2004), Identification of rice root associated nitrate, sulfate and ferric iron reducing bacteria during root decomposition, *FEMS Microbiol. Ecol.*, *50*, 101–110, doi:10.1016/j.femsec.2004.06.001.

Shi, J. B., L.-N. Liang, and G.-B. Jiang (2005), Simultaneous determination of methylmercury and ethylmercury in rice by capillary gas chromatography coupled on-line with atomic fluorescence spectrometry, *J. AOAC Int.*, *88*, 665–669.

Siciliano, S. D., N. J. O'Driscoll, R. Tordon, J. Hill, S. Beauchamp, and D. R. S. Lean (2005), Abiotic production of methylmercury by solar radiation, *Environ. Sci. Technol.*, *39*, 1071–1077, doi:10.1021/es048707z.

Slowey, A. J., and G. E. Brown (2007), Transformation of mercury, iron, and sulfur during the reductive dissolution of iron oxyhydroxide by sulfide, *Geochim. Cosmochim. Acta*, *71*, 877–894, doi:10.1016/j.gca.2006.11.011.

Spry, D. J., and J. G. Wiener (1991), Metal bioavailability and toxicity to fish in low-alkalinity lakes: A critical review, *Environ. Pollut.*, *71*, 243–304, doi:10.1016/0269-7491(91)90034-T.

Standard Methods Committee (1998), *Standard Methods for the Examination of Water and Wastewater*, 20th ed., Am. Pub. Health Assoc./Am. Water Works Assoc./Water Environ. Fed., Washington, D. C.

St. Louis, V. L., J. W. M. Rudd, C. A. Kelly, K. G. Beaty, N. S. Bloom, and R. J. Flett (1994), Importance of wetlands as sources of methyl mercury to boreal forest ecosystems, *Can. J. Fish. Aquat. Sci.*, *51*, 1065–1076, doi:10.1139/f94-106.

Ullrich, S., T. Tanton, and S. Abdrashitova (2001), Mercury in the aquatic environment: A review of factors affecting methylation, *Crit. Rev. Environ. Sci. Technol.*, *31*, 241–293, doi:10.1080/20016491089226.

Ulrich, P. D., and D. L. Sedlak (2010), Impact of iron amendment on net methylmercury export from tidal wetland microcosms, *Environ. Sci. Technol.*, *44*, 7659–7665, doi:10.1021/es1018256.

U.S. Environmental Protection Agency (EPA) (2001), Method 1630: Methyl mercury in water by distillation, aqueous ethylation, purge and trap, and cold vapor atomic spectrometry, *Rep. EPA-821-R-01-020*, 55 pp., U.S. Dep. of Int., Washington, D. C.

U.S. Environmental Protection Agency (EPA) (2002), Method 1631, Revision E: Mercury in water by oxidation, purge and trap, and cold vapor atomic fluorescence spectrometry, *Rep. EPA-821-R-02-019*, 46 pp., U.S. Dep. of Int., Washington, D. C.

U.S. Environmental Protection Agency (EPA) (2007), Method 7473: Mercury in solids and solutions by thermal decomposition, amalgamation, and atomic absorption spectrophotometry, *Rep. EPA-7473 (SW-846)*, 17 pp., U.S. Dep. of Int., Washington, D. C.

Windham-Myers, L., M. Marvin-DiPasquale, D. P. Krabbenhoft, J. L. Agee, M. H. Cox, P. Heredia-Middleton, C. Coates, and E. Kakouros (2009), Experimental removal of wetland emergent vegetation leads to decreased methylmercury production in surface sediment, *J. Geophys. Res.*, *114*, G00C05, doi:10.1029/2008JG000815.

Yu, R., J. R. Flanders, E. E. Mack, R. Turner, M. B. Mirza, and T. Barkay (2012), Contribution of coexisting sulfate and iron reducing bacteria to methylmercury production in freshwater river sediments, *Environ. Sci. Technol.*, *46*, 2684–2691, doi:10.1021/es2033718.

Zhang, H., X. Feng, T. Larssen, G. Qiu, and R. D. Vogt (2010), In inland China, rice, rather than fish is the major pathway for methylmercury exposure, *Environ. Health Perspect.*, *118*, 1183–1188, doi:10.1289/ehp.1001915.